

DESIGN AND SCREENING OF ANTIMICROBIAL PEPTOID LIBRARIES

By

Jeremy A. Turkett

A Thesis Submitted in Partial Fulfillment of the Requirements for the Degree of
Master of Science in Chemistry

Middle Tennessee State University

August 2017

Thesis Committee:

Dr. Kevin Bicker

Dr. Scott Handy

Dr. Justin Miller

ABSTRACT

Growing prevalence of antibiotic resistant bacterial infections necessitates the development of novel antimicrobials, which could be rapidly identified from combinatorial libraries. Peptoids are a class of antimicrobial peptidomimetics which are uniquely suited for library synthesis. The research presented utilizes the peptoid library agar diffusion (PLAD) assay¹ to screen peptoid libraries against the ESKAPE pathogens, including the optimization of assay conditions for each pathogen. Work presented here focuses on the tailoring of combinatorial peptoid library design through a detailed study of how peptoid lipophilicity relates to antibacterial potency and mammalian cell toxicity. The information gleaned from this optimization was then applied using the aforementioned screening method to examine the relative potency of peptoid libraries against *Staphylococcus aureus*, *Acinetobacter baumannii*, and *Enterococcus faecalis* prior to and following functionalization with long alkyl tails. The data indicate that overall peptoid hydrophobicity and not simply alkyl tail length is strongly correlated with mammalian cell toxicity.² The necessity of peptoid library lipophilicity being illuminated by the study, library development shifted to addressing the difficulties presented by single bead analysis via ESI tandem MS (MS/MS).

TABLE OF CONTENTS

LIST OF FIGURES.....	v
LIST OF TABLES.....	vii
CHAPTER ONE: INTRODUCTION.....	1
Modern Antibiotics.....	1
β -lactam Mechanism of Action.....	2
Bacterial Resistance.....	3
Alternative Antibiotics.....	4
Peptoids as Therapeutic Agents.....	7
Combinatorial Methods of Synthesis.....	8
Structural Elucidation of Peptoids.....	10
High-Throughput Screening.....	11
Project Aims.....	13
CHAPTER TWO: METHODS AND MATERIALS.....	15
Materials and Methods.....	15
Mono- <i>N</i> -Boc-cystamine.....	16
Mono- <i>N</i> -Boc-1,4-diaminobutane.....	16
Mono- <i>N</i> -Boc-1,2-diaminoethane.....	17
<i>N</i> -(aminoethyl)- <i>N'</i> - <i>N''</i> -bis-(<i>tert</i> -butoxycarbonyl)guanidine).....	18
Synthesis of 4x <i>N</i> -Mea for Branching Confirmation.....	18
Synthesis of Disulfide Linker.....	19
Combinatorial Library Synthesis.....	20
Synthesis of JTL1 ₁₀ and JTL1 ₁₃	21
Synthesis of JTL2.....	21
Peptoid Library Agar Diffusion (PLAD) Assay.....	22
ESKAPE Pathogen Growth Optimization.....	22
K15 Variant Synthesis (n=1, 3, 6, 8, 10, and 13).....	24

ESKAPE Panel.....	26
Minimum Inhibitory Concentration (MIC) Testing Against ESKAPE Pathogens.....	27
Hemolytic Assay.....	28
HepG2 Cytotoxicity Assay.....	29
Synthesis of Branched Linker.....	30
Synthesis of JTL3.....	31
CHAPTER THREE: RESULTS AND DISCUSSION.....	32
PLAD Assay Optimization for ESKAPE Pathogens.....	32
Synthesis of JTL1.....	34
Lipophilic Modification of K15.....	37
Lipophilic Modification of JTL1.....	46
Synthesis of JTL2.....	49
Synthesis of JTL3.....	50
Synthesis of Arginine Mimic.....	51
CHAPTER FOUR: CONCLUSION.....	53
REFERENCES.....	54

LIST OF FIGURES

Figure 1.1. β -lactam Antibiotics	1
Figure 1.2. β -lactam Mechanism of Action.....	2
Figure 1.3. β -lactamase Bacterial Resistance.....	3
Figure 1.4. AMP Mechanism of Action.....	5
Figure 1.5. Mammalian and Bacterial Membranes.....	6
Figure 1.6. Peptide v. Peptoid.....	7
Figure 1.7. Peptoid Synthesis.....	8
Figure 1.8. Split-and-Pool Synthesis.....	9
Figure 1.9. Peptoid Sequencing.....	11
Figure 1.10. PLAD Tag Molecule.....	12
Figure 1.11. PLAD Assay.....	13
Figure 3.1. Testing of TCEP Tolerance for the ESKAPE Pathogens.....	34
Figure 3.2. General Structures for the PLAD Linked Antibacterial Libraries JTL1, JTL1 ₁₀ and JTL1 ₁₃	36
Figure 3.3. The Structure of Variants of the K15 Antimicrobial Peptoid.....	37
Figure 3.4A. Structure and Linear MS of K15-1.....	38
Figure 3.4B. Structure and Linear MS of K15-3.....	39
Figure 3.4C. Structure and Linear MS of K15-6.....	39
Figure 3.4D. Structure and Linear MS of K15-8.....	40
Figure 3.4E. Structure and Linear MS of K15-10.....	40
Figure 3.4F. Structure and Linear MS of K15-13.....	41
Figure 3.5. Correlation Between Variant Alkyl Tail Length and Calculated Diffusion Coefficient	41
Figure 3.6. Growth Inhibition Profiles of the K15 Variants	43
Figure 3.7. Toxicity Profiles of the K15 Variants	44
Figure 3.8. Representative Images of the PLAD Screenings of Libraries JTL1, JTL1 ₁₀ , and JTL1 ₁₃	47

Figure 3.9. JTL2 Library Schematic.....	49
Figure 3.10. JTL3 Library Schematic	50
Figure 3.11. Cyclization of Propyl Di-Amine Arginine Mimic	52
Figure 3.12. N-(aminoethyl)-N'-N''-bis-(<i>tert</i> -butoxycarbonyl)guanidine).....	52

LIST OF TABLES

Table 2.1. Yields for K15 Variants.....	25
Table 3.1. Antibacterial Potency and Mammalian Cytotoxicity of K15 Variants.....	45

CHAPTER ONE: INTRODUCTION

Modern Antibiotics

The era of microbial therapeutics began with Alexander Fleming's discovery of penicillin in 1928. He observed the inhibition of *Staphylococcus aureus* in the presence of the mold *Penicillium notatum*. The active compound was isolated from the mold and used as a broad-spectrum antibiotic in the 1940s. During this time, penicillin underwent derivatization to modify pharmacokinetic and pharmacodynamic properties. By selectively substituting constituent functionalities, stability and efficacy were improved. Other natural products were sought for similar antimicrobial activity and structural similarities were found in the isolated active compounds. A major feature common in many natural product antibiotics is the β -lactam ring (Figure 1.1).³

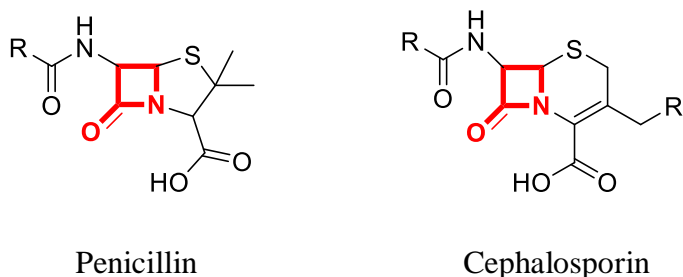


Figure 1.1 β -lactam Antibiotics. Structures highlight the four-membered β -lactam ring responsible for compound efficacy present in penicillin and cephalosporin derived antibiotics.

Treatment for infection has long relied on this class of compounds. In modern pharmaceuticals, β -lactam derived compounds account for 35% of the \$55 billion-dollar antibiotic market in the United States alone.³

β -lactam Mechanism of Action

The mode of action for β -lactam drugs is the inhibition of the enzymes responsible for the final stages of membrane construction. The targeted penicillin-binding proteins (PBPs) often exhibit bifunctionality, that of transpeptidase and transglycosylase, and assist in the synthesis of the cell membrane by extending the membrane constituent polymeric chain. β -lactam drugs will bind to the serine in the enzymatic active site of the PBPs, effectively deactivating them. The disruption in membrane synthesis weakens it and is shed when the affected microbe undergoes cell division. A spheroplast, an unbound cell, results from binary fission, and the bacterium is lysed in hydrophilic regions of the surrounding environment (**Figure 1.2**).⁴

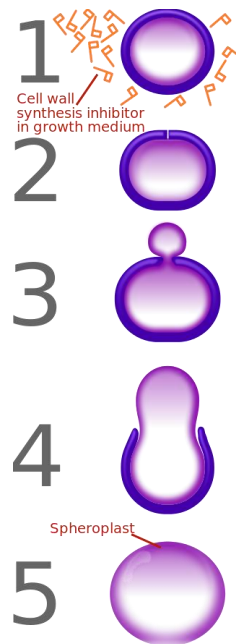


Figure 1.2 β -lactam Mechanism of Action. Schematic showing general mode of initiating cell death.

Replication is a rapid, exponential process for many pathogens, approximately 30 minutes for *S. aureus* to double in population. Because of this, halting cell reproduction is an efficient mode to control bacterial growth.⁵

Bacterial Resistance

Microbes regularly exposed to antibacterial compounds develop mechanisms of resistance. In response to generations of dependence on β -lactam antibiotics, bacteria have developed two primary mechanisms for resistance.⁴ The first are enzymes penicillinase and β -lactamase which target the β -lactam ring ubiquitous in penicillin derived bactericides and hydrolyze at the amide bond, opening the characteristic ring. The compound then undergoes decarboxylation and is thereafter inactive (**Figure 1.3**).

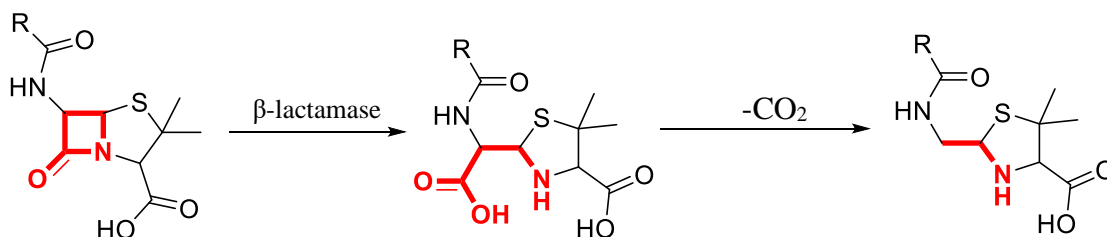


Figure 1.3 β -lactamase Bacterial Resistance. Structure showing enzymatic hydrolysis of the β -lactam ring in a penicillin derivative.

A more common mechanism for Gram-negative bacteria is the *mecA* gene. This gene encodes for the biosynthesis of PBPs for which β -lactams have a diminished binding affinity, and the antibiotic is rendered ineffective.³ These defenses against penicillin and its derivatives are only a few of the existing forms of bacterial resistance. Glycopeptides like Vancomycin have been

observed to be less effective against strains which have developed a thicker cell membrane to ameliorate or altogether halt the interference caused by the drug.⁴

Multiple drug resistant (MDR) bacteria are increasingly common and present a global threat to modern healthcare. The World Health Organization published a report in 2014 which indicate the deleterious effect the MDR epidemic has on mortality rate and economic growth. It stated that by 2050, 10 million premature deaths per year and a loss of \$100 trillion dollars in worldwide economic damages would be the result of this growing problem.⁶ Many MDR strains are common to hospitals, chiefly methicillin resistant *S. aureus* (MRSA), where bacterial infection could be fatal to immunosuppressed patients receiving care.⁷ Alone, MRSA was responsible for half of all nosocomial infections and 100,000 deaths in a 2014 study.^{3,6} It is clear that new antibiotics effective against MDR pathogens are needed. One class of alternative antibiotics which has garnered interest is antimicrobial peptides.

Alternative Antibiotics

Antimicrobial peptides (AMPs) occur naturally as part of innate immune response in many organisms which are capable of staving off bacterial, fungal, and viral infections. Peptides are amino acid chains linked by an amide or peptide bond. The amino acid residues have R groups of varying functionality.⁸ The secondary structure is determined by intramolecular interactions, such as hydrogen bonding between the carbonyl oxygen and the hydrogen of the amide nitrogen. Both the folding of the peptide and the chemical properties of included side-chains determine the function and efficacy of the compound. The wide-spectrum efficacy of AMPs is in part due to the non-specific membrane interactions by which they kill foreign bodies in the host.⁹ AMPs are

commonly cationic and amphipathic (having regions of hydrophobicity and hydrophilicity). The proposed mechanism is largely driven by electrostatic attraction between the partially negative bacteria membrane and partially positive amino acid side-chains in the AMP. The folded peptide will orient the charge centers to face the membrane. Once situated, weaker hydrophobic interactions will take place. The AMP will then insert itself in the membrane, creating a pore. The mechanism will proceed with self-promoted uptake, pulling in more AMPs which then interfere with vital processes within the cell. Alternatively, more pores form, leading to destruction of the membrane and ultimately cell death (**Figure 1.4**).¹⁰

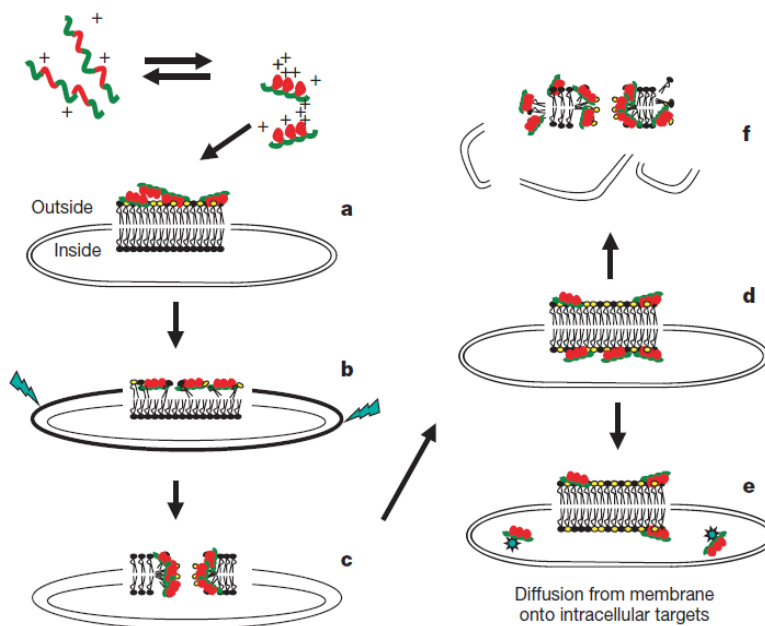


Figure 1.4 AMP Mechanism of Action. Representation of proposed method of AMP cell death. (a) peptide folding and orientation, (b) peptide-membrane electrostatic attraction, (c) hydrophobic interaction and pore formation, (d) AMP permeation through membrane, (e) attack of intracellular molecules, (f) lysis of membrane.¹⁰

The drawback to AMPs as therapeutics is threefold: toxicity, stability, and cost. Though the proposed mode of action for AMPs indicates a greater preference for the bacteria membrane than mammalian because of electrostatic interactions, the structure of AMPs is like nuclear localization signal peptides (**Figure 1.5**).

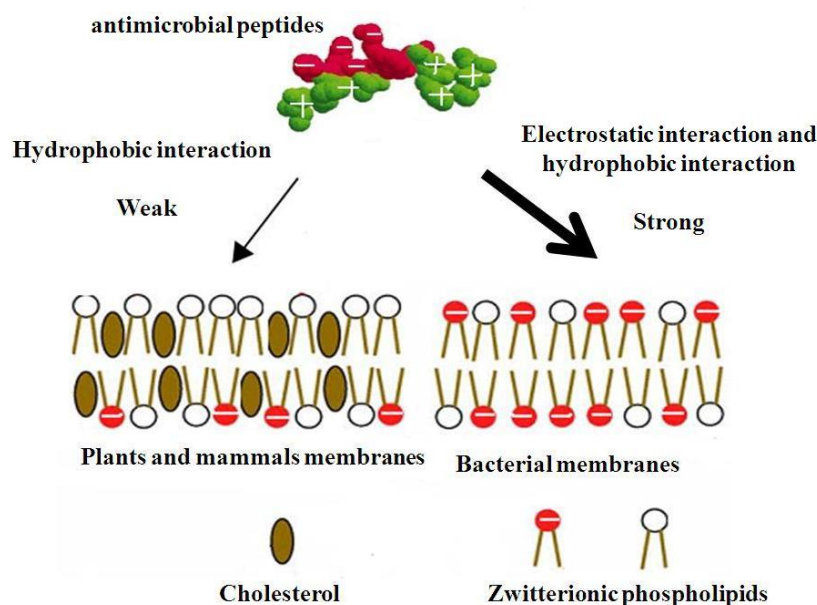


Figure 1.5 Mammalian and Bacterial Membranes. Selectivity of AMPs for bacteria cells over mammalian and plant cells due to strength of electrostatic attraction in bacterial membrane interactions.⁹

The signal peptides can move into the cell with ‘passenger’ molecules to the nucleus. Shared characteristics between the two has the potential for host cytotoxicity. AMPs are easily recognized and broken down by proteases in protein regulation and reclamation of amino acids for the host’s use. This is largely due to the peptide linkage which forms the compound backbone. Proteolytic instability significantly limits bioavailability, having a direct impact on drug efficacy. Additionally, amino acid building blocks needed for the synthesis of AMPs are prohibitively

costly. It is for these reasons peptidomimetics have emerged as a more likely candidate for therapeutic development.⁹

Peptoids as Therapeutic Agents

Peptoids are N-substituted glycine mimics of peptides that are structurally similar to peptides but the side-chain is anchored on the amide nitrogen rather than the α -carbon (**Figure 1.6**).



Figure 1.6 Peptide v. Peptoid. Structures showing the R group shift in peptide and peptoid backbones.

The transposition of the R group limits the ability of proteases to cleave the amide bonds in the compound's backbone, increasing bioavailability.^{11,12} Despite this structural alteration, peptoids possess similar chemico-physical properties to AMPs, namely a net positive charge and amphipathicity. They have demonstrated antimicrobial potency against a variety of pathogens including *Mycobacterium tuberculosis* and *Pseudomonas aeruginosa*.¹³⁻¹⁶

The synthesis of peptoids begins with the acylation of a free amine by bromoacetic acid activated by diisopropylcarbodiimide (DIC). The primary amine to be coupled is added and then displaces the bromine in an S_N2 reaction. This sequence of reactions forms the fundamental

building block of a peptoid, termed a submonomer. This can be repeated until the desired composition is achieved (**Figure 1.7**).¹⁷

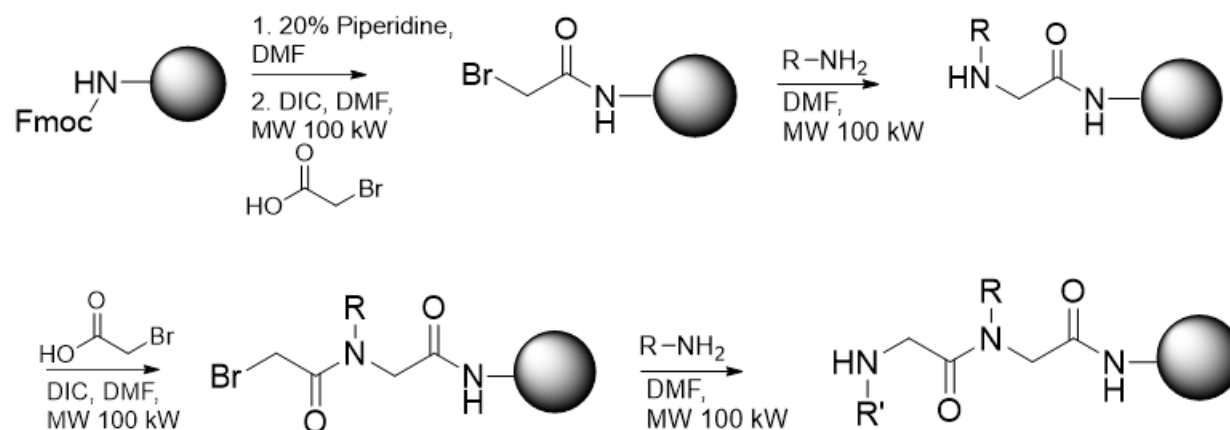


Figure 1.7 Peptoid Synthesis. Schematic showing the ‘submonomer’ stepwise synthesis of peptoids.

The primary amines introduced in the second stage of peptoid coupling are commercially available possessing a wide range of functionalities, providing for varied side chain properties. Where the peptide residues in synthetic AMPs are costly, even complex heterocyclic primary amines are less than a tenth the price per gram.

Combinatorial Methods of Synthesis

Zuckerman and his group introduced the technique of solid phase synthesis to the production of peptoids.¹⁷ By employing a solid phase resin with a terminal free amine, it is then possible to closely control the stepwise method of synthesis elucidated above. As the interface on which the compound is constructed is easily separated from the reaction solution, combinatorial

methods are able to be implemented into the regular process of synthesis. The most commonly used combinatorial technique is termed 'split-and-pool' synthesis (**Figure 1.8**).

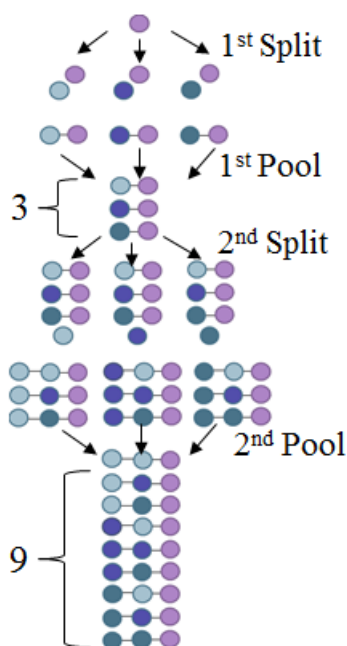


Figure 1.8 Split-and-Pool Synthesis. Schematic showing combinatorial synthesis with three submonomers and two couplings.

In this procedure, the beads are acylated, separated, and coupled with different amines. They are then collected and the steps of acylation, splitting, and coupling are repeated. Combinatorial synthesis is an efficient means of generating large diverse libraries of compounds.¹⁸ Given ten submonomers that are coupled four times using this technique, the theoretical diversity of the library will be 10^4 unique compounds.¹⁹ The structure of the member molecules is unknown at the time of synthesis. A means of analysis is required to later determine the composition of these compounds.

Structural Elucidation of Peptoids

The structural similarities between peptoid and peptide backbone composition allow sequencing via tandem mass spectrometry (MS) to be applied to N-substituted glycines. Tandem MS analysis proceeds by five steps: ionization, parent peak mass-to-charge (m/z) separation, fragmentation, ion speciation, and structural elucidation. Ionization provides a positive or negative charge to the analyte which allows identification by m/z and subsequent separation. In peptoids, the terminal amine nitrogen can bear a positive charge giving the compound a net positive charge. Fragmentation of the analyte occurs at predictable intervals along the backbone, cleaving at the N-terminus of the parent molecule to create a b-ion and leaving behind a y-ion. The energy of the fragmentation source is incrementally raised such that the next amide bond is broken, creating a new b-ion and y-ion. Proceeding in this manner for the number of couplings performed, it is possible to determine the peptoid structure by relating the difference in the unfragmented compound mass and the y-ion to that of the b-ion. An example of this process is shown in **Figure 1.9**.

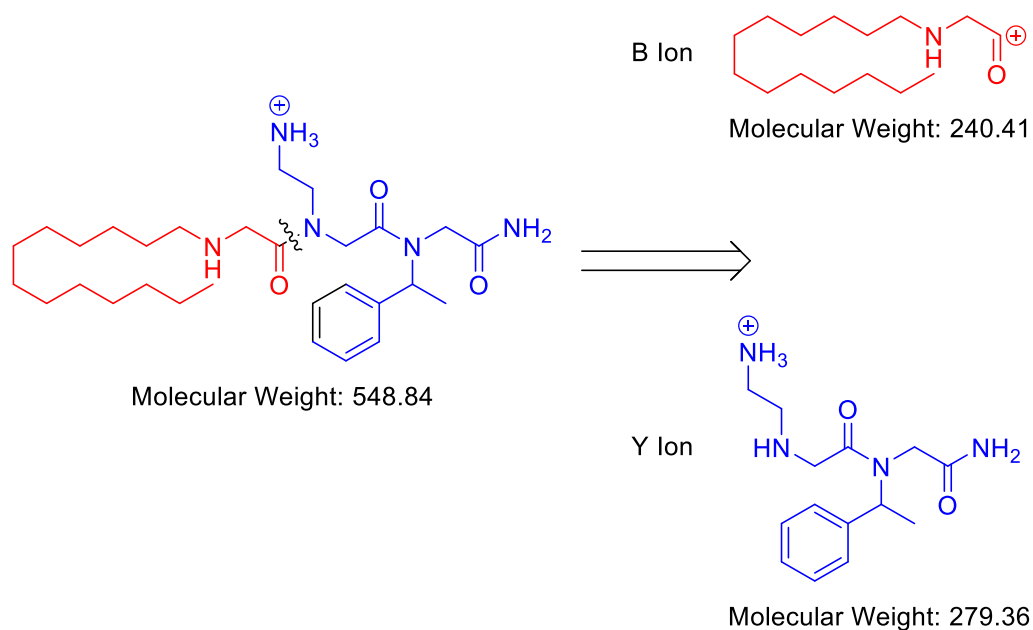


Figure 1.9 Peptoid Sequencing. Structures showing an example compound and ion speciation used in sequence determination of peptoids.

The mass of the ionized parent molecule (**Figure 1.9**) is 518.41 Da. After fragmentation at the N-terminus, the y-ion has a mass of 279.18 Da. The difference gives 239.23 Da which corresponds to the expected mass of the b-ion with an ionizing proton and thereby identifies the constituent submonomer.

High-Throughput Screening

The Bicker lab has developed a high-throughput assay for the screening of peptoid combinatorial libraries which employs a novel branched tag molecule.¹ The tag molecule allows for the synthesis of two identical peptoid strands (**Figure 1.10**).

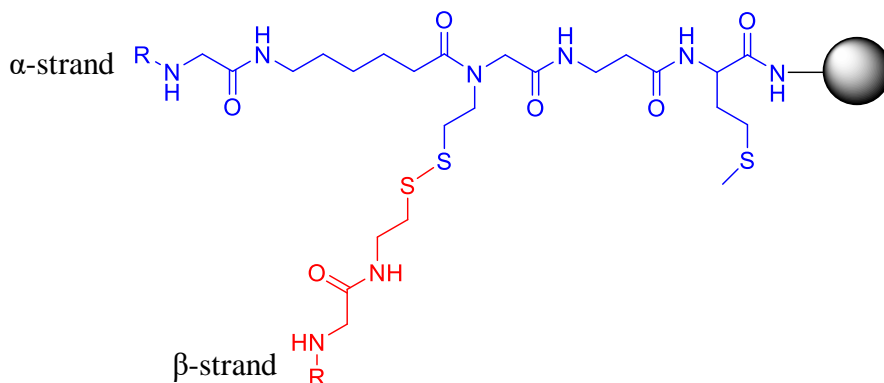


Figure 1.10 PLAD Tag Molecule. Structure showing branched linker used in PLAD assay with α -strand and β -strand labeled.

The β -strand is cleaved by treatment with a reducing reagent, and the α -strand with cyanogen bromide. In the Peptoid Library Agar Diffusion (PLAD) assay, an aliquot of the solid phase bound combinatorial library is combined with bacteria inoculant and reducing reagent. The mixture is poured over an agar plate and incubated overnight such that the inoculant can grow a uniform lawn. When exposed to the reducing reagent, the β -strand is freed from the resin and permeates into the surrounding agar. Compounds having antimicrobial potency will present with a zone of inhibition around the solid phase (**Figure 1.11**).

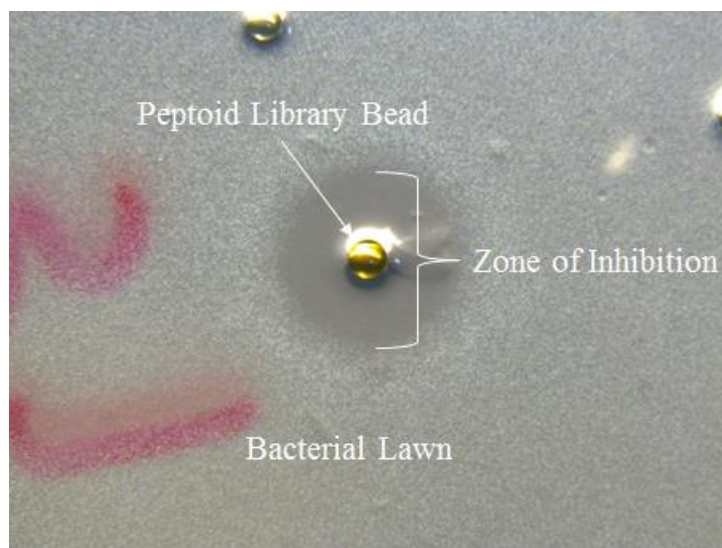


Figure 1.11 PLAD Assay. Pictured is a zone of inhibition around the solid phase resin, indicating an antimicrobial peptoid sequence.

These are removed from the plate, and the α -strand cleaved for sequencing via tandem mass spectrometry. Once the structure is determined, the peptoid is resynthesized on a larger scale for quantitative measurement of bioactivity by assessing the minimum inhibitory concentration (MIC) and cytotoxicity. The MIC is the concentration at which no bacterial growth is observed. This metric is then used to determine an appropriate concentration range to assay the cytotoxicity *in vitro*.¹

Project Aims

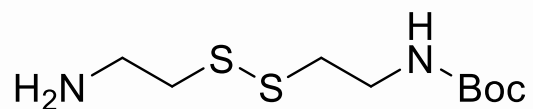
The goal of this project is twofold: the optimization of the PLAD assay for an expanded panel of screened pathogens and the improvement of antimicrobial potency in the generated peptoid libraries. The first component of which was the analysis and tailoring of the PLAD assay procedure to the growth conditions necessary for the clinically relevant ESKAPE panel consisting

of Gram-positive *Staphylococcus aureus*, *Enterococcus faecalis*, *Enterococcus faecium* and the Gram-negative *Escherichia coli*, *Klebsiella pneumoniae*, *Acinetobacter baumannii*, *Pseudomonas aeruginosa*. Library design was probed by the modification of a parent compound with alkyl tails of varying lengths. The resultant group of compounds were analyzed for increased potency and cytotoxicity which were then correlated to the physicochemical properties of the alkylated library.

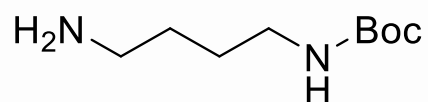
CHAPTER TWO: METHODS AND MATERIALS

Materials and Methods

Chemicals for the current work were purchased from Fisher Scientific (Waltham, MA), Alfa Aesar (Haverhill, MA), Amresco (Solon, OH), TCI America (Portland, OR), Anaspec (Fremont, CA), EMD Millipore (Billerica, MA), Peptides International (Louisville, KY), and Chem-Impex (Wood Dale, IL). Human red blood cells were purchased from Innovative Research (Novi, MI). Non-pathogenic *S. aureus*, ATCC 29213; *K. pneumoniae*, ATCC 7000603; *A. baumannii*, ATCC 19606; *P. aeruginosa*, ATCC 27853; *E. faecalis*, ATCC 29212; and *E. faecium*, ATCC 19434 were provided by Dr. Mary Farone in the Department of Biology at Middle Tennessee State University (MTSU). All mass spectra were acquired on a Waters Synapt HDMS QToF with Ion Mobility Mass Spectrometer. Spectrophotometric data acquired on Molecular Devices SpectraMax 5 Spectrophotometer. All images were acquired using a Leica M165FC stereoscope and were analyzed via Adobe Photoshop and Microsoft Excel. LogP, LogS, and LogD_{7.4} calculated using ChemAxon's MarvinSketch Calculator Plugins.

Mono-N-Boc-cystamine

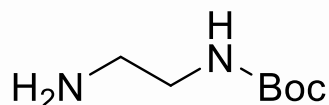
Cystamine dihydrochloride (5.9 g, 26.67 mmol) was dissolved in methanol (300 mL) and cooled to 0°C. Triethylamine (Et₃N, 11.2 mL, 80.01 mmol) was added to the solution and stirred for 30 minutes. Boc-anhydride (6.13 mL, 26.67 mmol) was added dropwise over 10 minutes then allowed to stir for 1 hour. The solution was concentrated *in vacuo*, producing a thick off-white residue. The product was then washed with diethyl ether (3x 30mL). 1 M sodium hydroxide (NaOH, 100 mL) was added to the residue and extracted twice with dichloromethane (DCM, 200 mL). Collected organic layers were combined and washed twice with water. The organic layer was dried over calcium chloride and concentrated *in vacuo* to yield a slightly yellow powdery solid (5.64 g, 83.8%). Boc-protection was confirmed by coupling with Rink Amide immobilized 4xNMea. An aliquot of the resin (50 mg) was acylated with 2 M Bromoacetic acid (1 mL, 2 mmol) and 3.2 M DIC (1 mL, 3.2 mmol) followed by coupling with a 1 M solution of the boc-protected product (1 mL, 1 mmol). ESI [M+H]⁺ expected: 785.99 observed: 785.2.

Mono-N-Boc-1,4-diaminobutane

Concentrated hydrochloric acid (HCl, 6.68 mL, 80.0 mmol) was added to methanol (100 mL) and cooled to 0°C. 1,4-diaminobutane (7.052 g, 80.0 mmol) was added to the acidified methanol and mixed for 20 minutes. De-ionized water (16.42 mL) was added and stirred for 30 minutes. Boc-anhydride (26.24 g, 120 mmol) in methanol (60 mL) was added dropwise over 10

minutes and stirred for 1 hour. Methanol was evaporated *in vacuo*, resulting in a white solid. The product was washed with diethyl ether (3x 30 mL). 1 M NaOH (100 mL) was added and the product extracted 2x with DCM (200 mL). The collected organic layers were combined and washed once with brine (100 mL). The organic layer was dried over calcium chloride and concentrated *in vacuo* overnight. The product was a white, powdery solid. (11.4 g, 75.8%). Boc-protections was confirmed by coupling with Rink Amide immobilized 4xNMea. An aliquot of the resin (50 mg) was acylated with 2 M Bromoacetic acid (1 mL, 2 mmol) and 3.2 M DIC (1 mL, 3.2 mmol) followed by coupling with a 1 M solution of the boc-protected product (1 mL, 1 mmol). ESI [M+H]⁺ expected: 721.98 observed: 721.8.

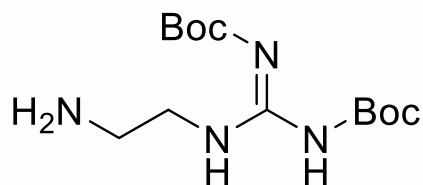
Mono-N-Boc-1,2-diaminoethane



Concentrated HCl (8.35 mL, 100.0 mmol) was added to methanol (100 mL) and cooled to 0°C. 1,2-diaminoethane (6.01 g, 100.0 mmol) was added to the acidified methanol and mixed for 20 minutes. De-ionized water (20.5 mL) was added and stirred for 30 minutes. Boc-anhydride (30.61, 150 mmol) in methanol (68 mL) was added dropwise over 10 minutes and stirred for 1 hour. Methanol was evaporated *in vacuo*, resulting in a white solid. The product was washed with diethyl ether (3x 30 mL). 1 M NaOH (100 mL) was added and the product extracted 2x with DCM (200 mL). The collected organic layers were combined and washed once with brine (100 mL). The organic layer was dried over calcium chloride and concentrated *in vacuo* overnight. The product was a white, powdery solid. (13.99 g, 87.4%). Boc-protections was confirmed by coupling with Rink Amide immobilized 4xNMea. An aliquot of the resin (50 mg) was acylated with 2 M

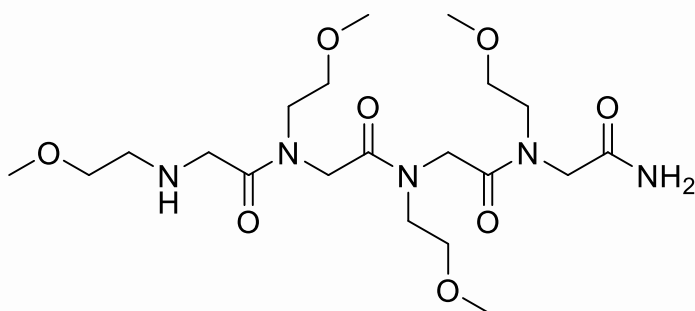
Bromoacetic acid (1 mL, 2 mmol) and 3.2 M DIC (1 mL, 3.2 mmol) followed by coupling with a 1 M solution of the boc-protected product (1 mL, 1 mmol). ESI $[M+H]^+$ expected: 693.93 observed: 693.8.

N-(aminoethyl)-N'-N''-bis-(tert-butoxycarbonyl)guanidine



Synthesis proceeded as described by 1,2-diaminoethane (0.961 g, 16.0 mmol, 4 eq.) was added to diisopropylethylamine (1.690 g, 13.08 mmol, 3.27 eq.) in 20 mL tetrahydrofuran. *N,N'*-bis(tert-butoxycarbonyl)-1H-pyrazole-1-carboxamide (1.24 g, 4.0 mmol, 1 eq.) was added dropwise over 6 hours to the diamine solution, then stirred for 18 hours. The solution was concentrated *in vacuo* overnight, yielding a resinous yellow solid (0.988 g, 78.1%). ESI $[M+H]^+$ expected: 103.2 observed: 103.5.

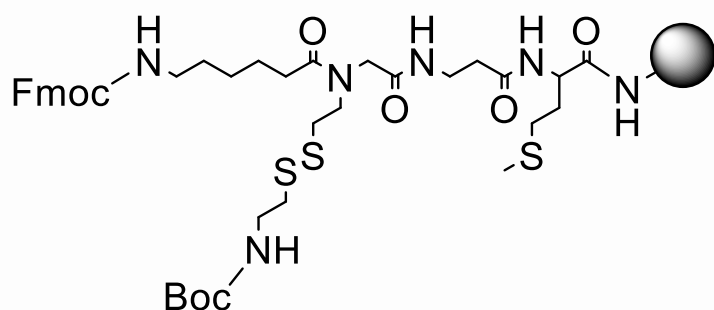
Synthesis of 4x N-Mea for Branching Confirmation



511 mg of Rink Amide resin (0.32 mmol/g loading capacity, total of 0.164 mmol) were swollen in dimethyl formamide (DMF) for 20 minutes. The Fmoc protecting group was removed from the resin by two treatments with 20% piperidine/DMF (v/v) for ten minutes. The first

coupling was performed by adding 3 mL 2 M bromoacetic acid in anhydrous DMF and 3 mL 3.2 M *N,N'*-diisopropylcarbodiimide (DIC) to the resin (total volume 6 mL), microwaved twice in a 1000 kW commercial microwave at 10% power (100 kW) for 15 seconds, and rocked for 20 minutes. Methoxyethylamine (901.3 mg, 1.031 mL, 12 mmol) was added to 4.97 mL anhydrous DMF, microwaved at 10% power twice for 15 seconds, and rocked for 30 minutes. The subsequent three couplings were performed under identical conditions. All reactions were tested with ninhydrin color test, and after each reaction the resin was washed 3x with DMF.

Synthesis of Disulfide Linker



1.0935 g of TentaGel macrobeads (0.25 mmol/g loading capacity, total of 0.273 mmol) were swollen in DMF for 20 minutes. The Fmoc protecting group was removed from the resin by two treatments with 20% piperidine/DMF (v/v) for ten minutes. Fmoc-methionine-OH (0.4062 g, 1.0935 mmol, 4 eq.) was activated with (1-cyano-2-ethoxy-2-oxoethylideneaminoxy)dimethylamino-morpholino-carbenium hexafluorophosphate (COMU, 0.4683 g, 1.0935 mmol, 4 eq.) for 10 minutes in 5% *N*-methylmorpholine (NMM)/DMF (v/v) for 10 minutes before being added to the swollen resin to react for 1 hour with gentle rocking. The Fmoc protecting group was removed from methionine by two treatments with 20% piperidine/DMF for ten minutes. Fmoc- β -alanine-OH (0.3404 g, 1.0935 mmol, 4 eq.) was activated with COMU (0.4683 g, 1.0935 mmol, 4 eq.) in 5% NMM/DMF for 10 minutes before

being added to the resin to react for 1 hour with gentle rocking. The Fmoc protecting group was removed from β -alanine by two treatments with 20% piperidine/DMF for ten minutes. 8 mL 2 M bromoacetic acid in anhydrous DMF and 8 mL 3.2 M DIC in anhydrous DMF were added to the resin (total volume 16 mL), microwaved twice in a 1000 kW commercial microwave at 10% power (100 kW) for 15 seconds, and rocked for 20 minutes. Boc-cystamine (8.0765 g, 32 mmol, 29.3 eq.) was added to 16 mL anhydrous DMF, microwaved at 10% power twice for 15 seconds, and rocked overnight. Fmoc-6-aminohexanoic acid (0.3863 g, 1.0935 mmol, 4 eq.) was activated with COMU (0.4683 g, 1.0935 mmol, 4 eq.) for 10 minutes in 5% NMM/DMF before being added to the resin to react for 1 hour with gentle rocking. All reactions were tested with ninhydrin color test, and after each reaction the resin was washed 3x with DMF.

Combinatorial Library Synthesis

Deprotection of disulfide linker modified TentaGel macrobeads (0.505 g) was achieved in a 20 mL fritted column by treating with 10 mL of 95% trifluoroacetic acid (TFA), 2.5% water, and 2.5% triisopropylsilane (TIS) for 1 h to remove Boc groups. The beads were washed in DMF 3x. This was followed by another deprotection reaction to remove Fmoc groups with 10 mL of 20% piperidine in DMF reacted for 20 min and repeated once more. The beads were washed 3x in DMF. The library was prepared using standard split-and-pool techniques¹⁸ by treating the deprotected resin with bromoacetic acid (1.39 g; 10 mmol) in anhydrous DMF (5 mL) and DIC (2.5 mL, 16 mmol) in anhydrous DMF (2.5 mL). The beads in solution were microwaved twice with a commercial microwave at 10% power (100 kW) for 15 s, agitating between steps. The reaction was rocked for 30 min, then the solution was aspirated and the beads washed 3x with DMF. Resin was resuspended in DMF, divided evenly into eight reaction vessels, and excess DMF was

removed. Each vial was treated with a different amine solution (2 mL; 2 M) in anhydrous DMF. The amines used were (isopropylamine (NVal), isobutylamine (NLeu), hexylamine (NHex), phenylethylamine (NPea), furfurylamine (NFur), tryptamine (NTrp), N-boc-1,4-diaminobutane (NLys), and N-boc-1,2-diaminoethane (NDae)). The vials were microwaved twice at 10% power (100 kW) for 15 s, agitating between steps. They were rocked for 30 minutes, then pooled together into the original 20 mL fritted synthesis column. The solution was aspirated and the beads washed 3x with DMF. The bromoacetic acid/DIC, splitting, amine coupling, and pooling steps were repeated three times for a total of four couplings. All reactions were tested with ninhydrin color test, and after each reaction the resin was washed 3x with DMF.

Synthesis of JTL1₁₀ and JTL1₁₃

Combinatorial library synthesis proceeded as described above. Two aliquots (200 mg) were taken from the library, named JTL1, and acylated with 2 M bromoacetic acid (3 mL, 6 mmol) and 3.2 M DIC (3 mL, 9.6 mmol). The aliquots were microwaved twice at 10% power (100 kW) for 15 s, agitating between steps. One aliquot was treated with decylamine (JTL1₁₀) while the other was treated with tridecylamine (JTL1₁₃). These were deprotected by 5 mL TFA/TIS/H₂O solution, resulting in removal of the Boc group.

Synthesis of JTL2

Protected disulfide linker (250 mg) was treated with 5 mL TFA/TIS/H₂O solution to remove Boc group. The unprotected *beta*-strand was then acylated with 2 M bromoacetic acid (5 mL, 10 mmol) and 3.2 M DIC (5 mL, 16 mmol) followed by coupling with 2 M tridecylamine (5

mL, 10 mmol). The *alpha*-strand was removed by 5 mL 20% piperidine in DMF. Combinatorial synthesis proceeded as described above with the same eight submonomers, yielding a library of theoretical diversity 4096.

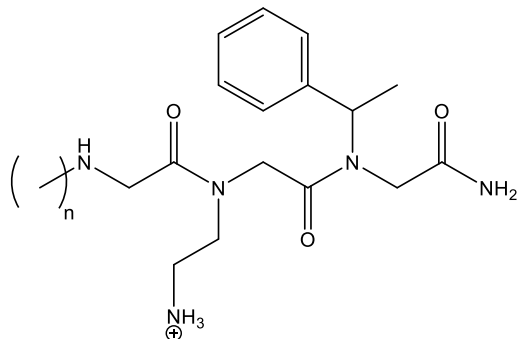
Peptoid Library Agar Diffusion (PLAD) Assay

Overnight cultures of the organism to be screened were started by collecting 1-3 separated colonies from an LB plate with a sterile loop and adding these to 3 mL of tryptic soy broth (TSB). Colonies were incubated for 18-24 hours at 37°C. TentaGel functionalized by peptoid library were deprotected with TFA/TIS/H₂O, then equilibrated in sterile water overnight. Soft agar (in aliquots of 3 mL) was heated to 100°C for 30 minutes, then cooled to 47°C. TentaGel was equilibrated in 500 µL phosphate buffered saline (PBS) for 30 minutes. 570 µL of a 100 mM reducing reagent solution (2-mercaptoethanol, BME, for *A. baumannii* and *P. aeruginosa*; Tris(2-carboxyethyl)phosphine hydrochloride, TCEP, for the remaining ESKAP pathogens), 500 µL of the PBS equilibrated resin, 75 µL of TSB bacteria culture, and 3 mL of the sterilized agar were combined and mixed 7-8 times. The mixture was poured onto a hard LB agar plate and swirled to evenly distribute. Solidified plates were incubated at 37°C for 6 hours for *S. aureus* and *K. pneumoniae* or 20 hours for the remaining ESKAPE pathogens. Zones of inhibition were measured with a Leica M165FC microscope.

ESKAPE Pathogen Growth Optimization

A tolerance study of the ESKAPE pathogens (*E. coli*, *S. aureus*, *K. pneumoniae*, *A. baumannii*, *P. aeruginosa*, *E. faecalis*, and *E. faecium*) was performed to assess degree of growth inhibition in the presence of TCEP, the reducing reagent shown to yield the largest zones of

inhibition. As the same study had already been performed on *E. coli*¹, it was not tested here. Separate lysogeny broth (LB) agar plates were streaked from the frozen stocks of the assayed pathogens and incubated at 37°C overnight. A sterile loop was used to collect 1-3 isolated colonies from the plates. The colonies were deposited in 5 mL tryptic soy broth (TSB) and incubated at 37°C overnight. The PLAD assay was performed as written with deviation allowing for the absence of TentaGel beads and reducing reagent. Briefly, two tubes of 3 mL soft LB agar were liquefied by boiling for each pathogen to be assayed (six) and cooled to 47°C. To this was added 75 µL of TSB bacteria stock for the organism analyzed, 500 µL PBS (to make up for the volume lost by the lack of beads), and 570 µL of either DI water (no TCEP control) or 100 mM TCEP (14 mM final). The tubes were gently mixed and poured on to an LB agar plate. All plates were incubated at 37°C overnight. Lawn density for each plate was assayed by Photoshop luminosity measurements of images from a Leica stereoscope. For *A. baumannii* and *P. aeruginosa* organismal growth was observed to have been inhibited in the presence of TCEP. These two organisms underwent an expanded study including two reducing reagents alongside TCEP at a range of concentrations. Dithiothreitol (DTT), BME, and TCEP were tested at 2, 4, 10, and 14 mM concentrations. These results led to the use of BME at 14 mM in the PLAD assay against *A. baumannii* and *P. aeruginosa*.

K15 Variant Synthesis (n=1, 3, 6, 8, 10, and 13)

Rink Amide resin (620.5 mg, 0.198 mmol) was deprotected by treatment with 20% piperidine in DMF twice for 20 min. 5 mL 2 M bromoacetic acid in anhydrous DMF and 5 mL 3.2 M DIC in anhydrous DMF were added to the resin (total volume 10 mL), microwaved twice at 10% power (100 kW) for 15 seconds, and rocked for 20 minutes. *N*-phenylethylamine (2.4236 g, 2.585 mL, 20 mmol) was added to 10 mL anhydrous DMF, microwaved at 10% power twice for 15 seconds, and rocked for 30 minutes. 5 mL 2 M bromoacetic acid in anhydrous DMF and 5 mL 3.2 M DIC in anhydrous DMF were added to the resin (total volume 10 mL), microwaved twice at 10% power (100 kW) for 15 seconds, and rocked for 20 minutes. *N*-(tert-butoxycarbonyl)-1,4-diaminobutane (3.2400 g, 20 mmol) was added to 10 mL anhydrous DMF, microwaved at 10% power twice for 15 seconds, and rocked for 30 minutes. An aliquot of this resin (103 mg) was placed into a separate synthesis column for later peptide coupling to produce K15-1. The rest of the resin was treated with 5 mL 2 M bromoacetic acid in anhydrous DMF and 5 mL 3.2 M DIC in anhydrous DMF (total volume 10 mL), microwaved twice at 10% power (100 kW) for 15 seconds, and rocked for 20 minutes. The acylated resin was divided into five equal portions which were then treated with an amine solution (2 M; 2 mL; in anhydrous DMF) to produce the appropriate K15 variant; tridecylamine (K15-13), decylamine (K15-10), octylamine (K15-8), hexylamine (K15-6), and propylamine (K15-3). These were microwaved twice for 15 seconds and rocked for

30 minutes, per standard procedure. The sixth unacylated portion was reacted with Fmoc-Sar-OH (46.07 mg, 0.148 mmol) and COMU (63.4 mg, 0.148 mmol) in 5 mL of 5% NMM for 1 h under gentle agitation. The solution was aspirated and the resin washed 3x with DMF. Fmoc protecting groups were removed by two treatments of 5 mL of 20% piperidine for 20 min. The six variants were cleaved from the bead by addition of 95% TFA, 2.5% H₂O, 2.5% TIS followed by gentle agitation for 1 h. The filtrate was collected and bubbled off until less than 1 mL remained. Each sample was diluted with 5 mL of acetonitrile and 5 mL of water. The peptoids were then purified individually by RP-HPLC on a C13 column using a gradient of water + 0.05% TFA to acetonitrile + 0.05% TFA. Solvent was removed *in vacuo* to yield each peptoid as a white powder. Yield and ESI-MS information are provided in the table below.

Table 2.1. Yields for K15 Variants

K15 Variant	Mass (in mg)	% Yield	Expected Mass	Observed Mass
1	3.9	15.2	350.22 Da	350.34 Da
3	2.8	18.3	378.25 Da	378.39 Da
6	8.1	52.2	420.30 Da	420.47 Da
8	9.6	58.2	448.33 Da	448.51 Da
10	9.8	55.7	476.36 Da	476.53 Da
13	11.3	58.8	518.41 Da	518.59 Da

ESKAPE Panel

For each of the bacterial strains to be screened, 1-3 isolated colonies were collected from a LB plate by a sterile loop and resuspended in 3 mL of TSB. The solutions were incubated at 37°C for 18-24 hours. After the growth period, the turbidity was measured at 600 nm and adjusted to an OD of 0.08-0.13 by diluting with TSB for an approximate concentration of 1×10^8 CFU/mL. Once the desired OD was achieved, 22.5 μ L of the bacteria suspension were diluted 1:20 in 427.5 μ L cation adjusted Mueller-Hinton broth (CAMHB) for a final concentration of 5×10^6 CFU/mL.

6 μ L of a 10 mM stock of the compound of interest were diluted in 534 μ L CAMHB for each bacterial strain assayed. 180 μ L of this solution were delivered to three wells (row A), which are to serve as the 100 from which the subsequent dilutions are taken. Rows B-H were filled with 90 μ L of broth. 90 μ L of the 100 μ M solution was withdrawn and delivered to the row below, resulting in a 1:2 dilution (100 to 50 mM, etc.) This was repeated for each dilution required, 7 for the current assay, with 90 μ L of the final triplicate set being removed such that each well has a volume of 90 μ L. 10 μ L of the 1:20 diluted bacteria were added to each well for a total volume of 100 μ L.

100 μ L of broth were delivered to a well in triplicate to serve as a media control. A tetracycline control was used in triplicate, composed of 4 μ L of 2 mg/mL antibiotic in 356 μ L broth with 40 μ L bacteria. 100 μ L of this solution were delivered to a well in triplicate.

The prepared plates were incubated for another 18-24 hours. Their respective absorbances at 600 nm were analyzed. 10 μ L of PrestoBlue were added to each well and allowed to incubate

for an hour. Their absorbances at 550, 570, 585 nm were analyzed to determine viable cells having survived treatment by the antimicrobial.

Minimum Inhibitory Concentration (MIC) Testing against ESKAPE Pathogens

For each of the bacterial strains screened, 1-3 isolated colonies were collected from a LB plate by a sterile loop and resuspended in 3 mL of TSB. The solutions were incubated at 37°C for 18-24 hours. After the growth period, the turbidity was measured at 600 nm and adjusted to an optical density (OD) of 0.08-0.13 by diluting with TSB for an approximate concentration of 1×10^8 CFU/mL. Once the desired OD was achieved, 20 μ L of the bacteria suspension were diluted 1:20 in 380 μ L Cation Adjusted Mueller-Hinton broth (CAMHB) for a final concentration of 5×10^6 CFU/mL.

4 μ L of a 10 mM stock of K15 were diluted in 356 μ L CAMHB for each bacterial strain assayed (a total of 28 μ L stock in 2.478 mL broth for ESKAPE panel). 180 μ L of this solution were delivered to three wells. For each dilution to be studied, 90 μ L of the 100 μ M solution were withdrawn and delivered to 90 μ L of broth. This 1:2 serial dilution was continued to give final K15 concentrations of 100, 50, 25, 12.5, 6.3, 3.1, and 1.6 μ g/mL. 90 μ L of the final triplicate set being removed such that each well has a volume of 90 μ L. A negative control containing 90 μ L of broth with no peptoid was also prepared. 10 μ L of the 1:20 diluted bacteria were added to each well for a total volume of 100 μ L. 100 μ L of broth were delivered to a well in triplicate to serve as a media control. A tetracycline control was used, composed of 4 μ L 2 mg/mL antibiotic in 356 μ L broth with 40 μ L bacteria. 100 μ L of this solution were delivered to each of three wells.

The prepared plates were incubated for another 18-24 hours. Their respective absorbance at 600 nm was analyzed on a SpectraMax M5 Plate Reader. 10 μ L of PrestoBlue were added to each well and allowed to incubate for an hour. Absorbance at 555, 570, and 585 nm was analyzed to determine viable cells having survived treatment by the antimicrobial compound. This assay, which utilizes triplicates of each K15 concentration, was ran in duplicate or triplicate for each microorganism tested on different days.

Hemolytic Assay

Compounds were tested at nine different concentrations of a 2-fold serial dilution (800-6.3 μ g/mL) along with a positive control (1% Triton-X100) and a negative control (vehicle) in triplicate. Briefly, 3.3 mL of human red blood cells (hRBCs) were pelleted from the commercial storage solution by centrifugation at 1000 rpm for 10 minutes. The supernatant was removed, and the cells resuspended in 10 mL of sterile PBS. Centrifugation, disposal of the supernatant, and resuspension in PBS was repeated twice more. The final resuspension was with 3.3 mL of sterile PBS. 100 μ L of the washed hRBCs were aliquoted to each necessary well of a 96-well plate. 11.1 μ L of the K15 variant peptoid compound in sterile PBS at 10x the concentration to be assayed were delivered to the designated wells. 11.1 μ L of sterile PBS were added to 3 wells for the negative control, and 11.1 μ L of 1% Triton-X100 detergent added to 3 wells for the positive control. The plate was incubated for 1 h at 37°C and centrifuged for 10 minutes at 1000 rpm. From each well, 5 μ L of the supernatant was transferred to 95 μ L of PBS in clear-bottomed 96-well plate and the absorbance read at 405 nm on a spectrophotometer. All triplicate assays were repeated twice on different days. Percent hemolysis was calculated as follows;

$$\% \text{ hemolysis} = \frac{(\text{OD}_{405\text{nm}} \text{ sample} - \text{OD}_{405\text{nm}} \text{ neg. control})}{(\text{OD}_{405\text{nm}} \text{ pos. control} - \text{OD}_{405\text{nm}} \text{ sample})} \times 100$$

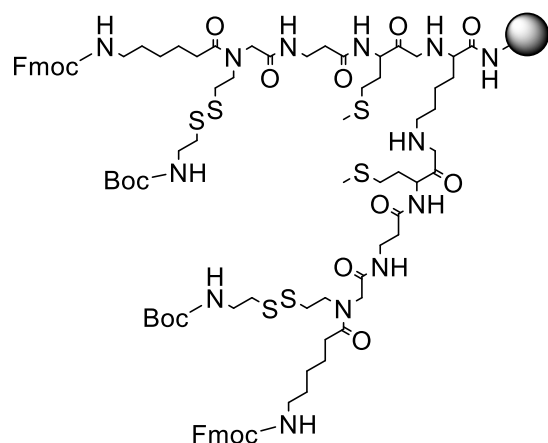
The Hill Slope (H) and HC_{50} was determined using GraFit and HC_{10} was calculated from HC_{50} using the following equation;

$$\text{HC}_{10} = \text{HC}_{50} [10\% / (100\% - 10\%)]^{1/H}$$

HepG2 Cytotoxicity Assay

Compounds were tested at nine different concentrations of a 2-fold serial dilution (800-6.3 $\mu\text{g}/\text{mL}$) along with a positive control (1% Triton-X100) and a negative control (vehicle) in triplicate. HepG2 cells were cultured in Dulbecco's Modified Eagle Medium (DMEM) supplemented with 10% FBS at 37 °C, 1% PSG, and 5% CO_2 atmosphere. For cytotoxicity testing, cells were seeded into 96-well plates (20,000-40,000 cells per well; 100 μL volume) in phenol red free DMEM containing 10% FBS and 1% PSG and incubated for 2 h to allow for cell attachment. Cells were then treated with varying concentrations of peptoid (2-fold serial dilution in PBS from 800-3.125 $\mu\text{g}/\text{mL}$) from 10x stocks in PBS. PBS alone and 1% Triton X-100 served as negative and positive controls, respectively. After 3 days incubation at 37°C, 20 μL of 5 mg/mL 3-(4,5-dimethylthiazol -2-yl)-2,5-diphenyltetrazolium bromide (MTT) was added to each well and incubated at 37°C for 3.5 h. Media was then removed and 100 μL dimethyl sulfoxide (DMSO) was added to lyse the cells and release the metabolized dye. The absorbance at 570 nm was then read on a spectrophotometer, percent inhibition determined, and IC_{50} calculated using GraFit. All triplicate assays were repeated three times on different days.

Synthesis of Branched Linker



159 mg of TentaGel macrobeads (0.25 mmol/g loading capacity, total of 0.04) were swollen in dimethyl formamide (DMF) for 20 minutes. The Fmoc protecting group was removed from the resin by two treatments with 20% piperidine/DMF (v/v) for ten minutes. Fmoc-lysine-MTT-OH (100.0 mg, 0.16 mmol, 4 eq.) was activated with COMU (68.1 mg, 0.16 mmol, 4 eq.) for 10 minutes in 5% NMM/DMF (v/v) for 10 minutes before being added to the swollen resin to react for 1 hour with gentle rocking. The Fmoc protecting group was removed from lysine by two treatments with 20% piperidine/DMF for ten minutes. The MTT protecting group was removed by treatment with 1% TFA in DCM. Fmoc-methionine-OH (59.1 mg, 0.16 mmol, 4 eq.) was activated with COMU (68.1 mg, 0.16 mmol, 4 eq.) for 10 minutes in 5% NMM/DMF (v/v) for 10 minutes before being added to the resin to react for 1 hour with gentle rocking. The Fmoc protecting group was removed from methionine by two treatments with 20% piperidine/DMF for ten minutes. Fmoc- β -alanine-OH (49.5 mg, 0.16 mmol, 4 eq.) was activated with COMU (68.1 mg, 0.16 mmol,

4 eq.) in 5% NMM/DMF for 10 minutes before being added to the resin to react for 1 hour with gentle rocking. The Fmoc protecting group was removed from β -alanine by two treatments with 20% piperidine/DMF for ten minutes. 3 mL 2 M bromoacetic acid in anhydrous DMF and 3 mL 3.2 M DIC in anhydrous DMF were added to the resin (total volume 6 mL), microwaved twice in a 1000 kW commercial microwave at 10% power (100 kW) for 15 seconds, and rocked for 20 minutes. Boc-cystamine (1.514 g, 6 mmol, 37.5 eq.) was added to 6 mL anhydrous DMF, microwaved at 10% power twice for 15 seconds, and rocked overnight. Fmoc-6-aminohexanoic acid (56.17 mg, 0.16 mmol, 4 eq.) was activated with COMU (68.1 mg, 0.16 mmol, 4 eq.) for 10 minutes in 5% NMM/DMF before being added to the resin to react for 1 hour with gentle rocking. All reactions were tested with ninhydrin color test, and after each reaction the resin was washed 3x with DMF.

Synthesis of JTL3

Protected branched disulfide linker (159 mg) was treated with 5 mL TFA/TIS/H₂O solution to remove Boc group. The unprotected *beta*-strand was then acylated with 2 M bromoacetic acid (5 mL, 10 mmol) and 3.2 M DIC (5 mL, 16 mmol) followed by coupling with 2 M tridecylamine (5 mL, 10 mmol). The *alpha*-strand was removed by 5 mL 20% piperidine in DMF. Combinatorial synthesis proceeded as described above with the same eight submonomers, yielding a library of theoretical diversity 4096.

CHAPTER THREE: RESULTS AND DISCUSSION

The overall goal of the work is to improve peptoid library design with regards to frequency of compound exhibiting a zone of bacterial growth inhibition and potency of compounds screened via the Peptoid Agar Library Diffusion (PLAD) assay. In pursuit of this objective, there were several intermediate stages of development; the first being combinatorial library synthesis, PLAD assay optimization for an expanded panel of pathogens, and library screening.² Observations made during screening led to a study of physicochemical properties of potent antimicrobial peptoids identified via our assay. Next, library design strategy was altered to address issues with sequencing potent compounds. Finally, preliminary work was performed for the inclusion of novel amine side-chains into peptoid libraries.

PLAD Assay Optimization for ESKAPE Pathogens

The PLAD assay has been used to identify compounds exhibiting antimicrobial properties against *E. coli* biofilms and *Cryptococcus neoformans*.^{20,21} We chose to expand our use of the PLAD assay to the clinically relevant ESKAPE panel of bacterial pathogens (*E. coli*, *S. aureus*, *K. pneumoniae*, *A. baumannii*, *P. aeruginosa*, *E. faecalis*, and *E. faecium*). This panel of microorganisms represents bacteria that are responsible for most drug-resistant infections.¹⁶ The first step towards PLAD screening of the ESKAPE pathogens was optimization of reducing

reagent conditions for each microorganism, which is responsible for release of the *beta*-strand peptoid from the PLAD linker. An ideal reducing reagent produces a noticeable zone of inhibition around effective beads without causing deleterious effects on bacterial lawn growth compared to a control with no reducing reagent. Procedurally, the PLAD assay involves mixing together melted soft agar media maintained at 47 °C, an aliquot of the library to be screened, a reducing reagent, and an inoculant of the microorganism of interest. This mixture is then poured onto a solid agar Petri dish, allowed to cool, and incubated for an optimal amount of time to produce a lawn of microorganism on the media. The modular setup of the PLAD assay allows us to quickly and easily evaluate several reducing reagents to determine the optimal assay conditions for each microorganism. Assay screening against the ESKAPE pathogens required minimal optimization; with only *A. baumannii* and *P. aeruginosa* requiring a change in reducing agent from 14 mM TCEP which had been previously shown to be effective in *beta*-strand peptoid cleavage from the PLAD linker (**Figure 3.1**).²⁰ *A. baumannii* and *P. aeruginosa* tolerance to varied concentrations of TCEP alongside two other reducing reagents, DTT and BME, was assayed (**Figure 3.1**). Optimal reducing reagent conditions for these microorganisms were determined to be 14 mM BME, which showed no deleterious effects on bacterial lawn growth.

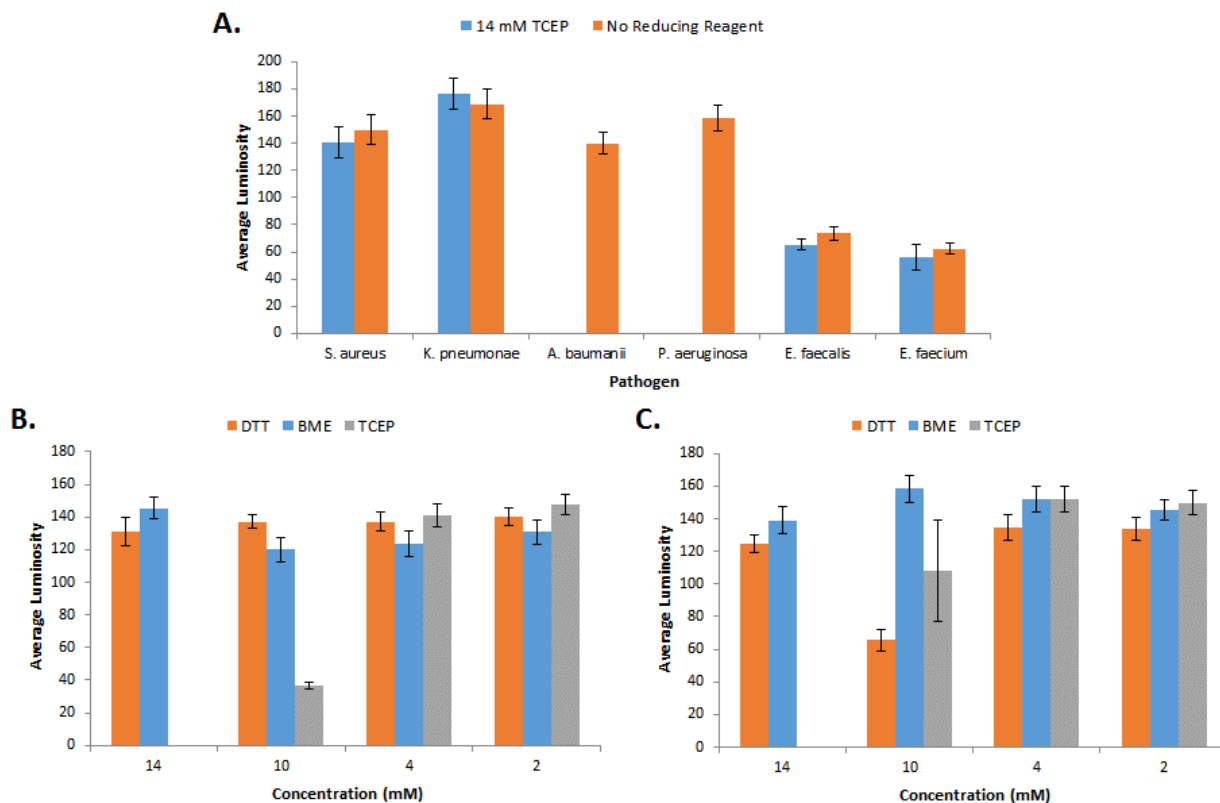
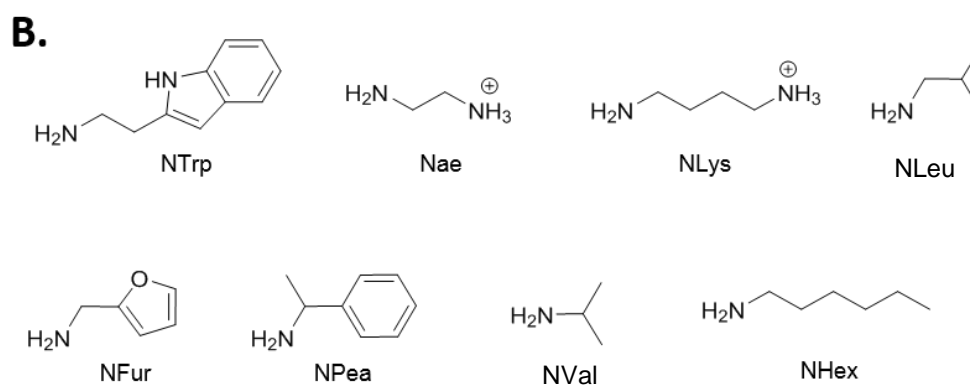
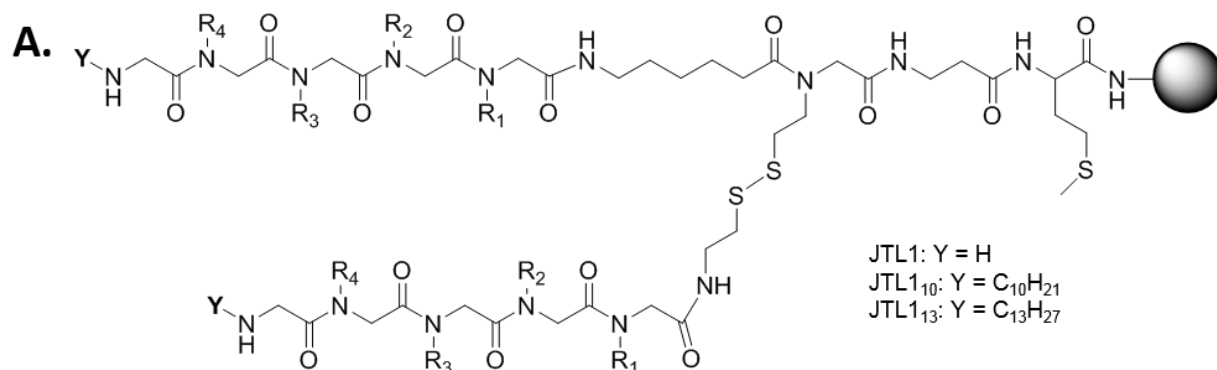


Figure 3.1. (A.) Testing of TCEP Tolerance for the ESKAPE Pathogens. (B.) Optimization of PLAD Assay Reducing Reagent for *A. baumannii*. (C.) Optimization of PLAD Assay Reducing Reagent for *P. aeruginosa*.

Synthesis of JTLL1

A combinatorial tetramer peptoid library, termed JTLL1 (**Figure 3.2A**), was synthesized to assess the efficacy of the PLAD assay in the varied bacteria panel. The library incorporated a mix of submonomers showing hydrophobic (isopropylamine (NVal), isobutylamine (NLeu), hexylamine (NHex)), aromatic (phenylethylamine (NPea), furfurylamine (NFur), tryptamine (NTrp)), and cationic characteristics (diaminobutane (NLys), diaminoethane (Nae)) (**Figure 3.2B**). The eight submonomers selected yielded a theoretical diversity of 4096 compounds. Split-

and-pool synthesis starting with 0.5 g TentaGel Macrobeads gave a total of roughly 33,000 individual beads, representing approximately eight replicates of the theoretical diversity. This built in replication was intentional, allowing us to in theory screen the entire diversity of JTL1 against each ESKAPE pathogen. The library was initially screened against *S. aureus*, a Gram-positive organism responsible for many nosocomial infections with excellent tolerance to PLAD assay conditions. However, screening of a significant portion of the theoretical diversity yielded no “hits,” or beads with measurable zones of inhibition (**Figure 3.2C**). This result, while not expected, was not without precedent. During concomitant experimentation in our lab using a similarly designed combinatorial library intended for screening against *C. neoformans* H99S, one bead of 39,300 presented a zone of inhibition.²¹ Furthermore, poor efficacy was observed for this hit upon resynthesis and traditional characterization. It was postulated that the lack of potent compounds was due to low lipophilicity, consistent with studies in which long alkyl tails have been correlated with improved antimicrobial activity.²² As such, we next sought to rapidly evaluate the utility of lipophilic moieties in JTL1 using the high-throughput nature of the PLAD assay.



C.

Library	<i>S. aureus</i>	<i>E. faecalis</i>	<i>A. baumannii</i>
JTL1	0%	0%	0%
JTL1 ₁₀	3.3%	8.8%	6.7%
JTL1 ₁₃	4.2%	16.7%	16.6%

Figure 3.2. (A.) General Structures for the PLAD Linked Antibacterial Libraries JTL1, JTL1₁₀ and JTL1₁₃. (B.) Submonomers Randomly Incorporated into the Library were Chosen to Display Aromatic, Hydrophobic, and Cationic Side Chains. (C.) Hit Rate for Each of the Libraries Against *S. aureus*, *E. faecalis*, and *A. baumannii*.

Lipophilic Modification of K15

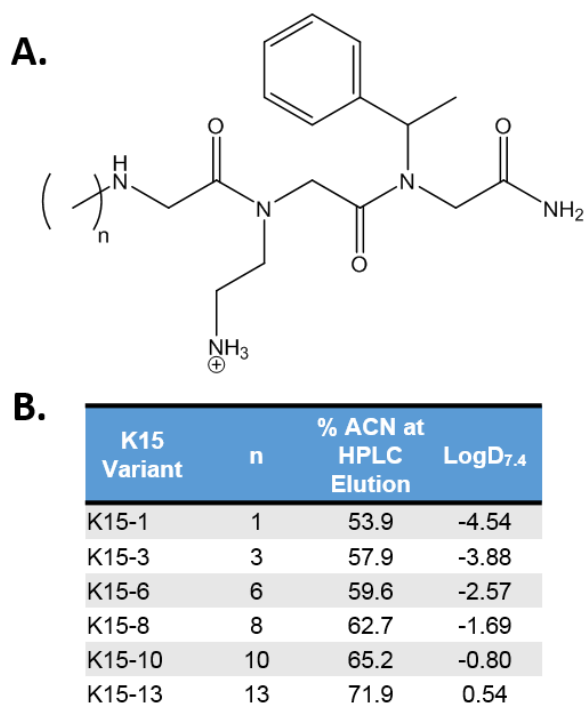


Figure 3.3. (A.) The Structure of Variants of the K15 Antimicrobial Peptoid Identified Previously with Varying Alkyl Tail Lengths on the N-terminus of the Peptoid. (B.) Structural, HPLC Hydrophobicity, and Diffusion Coefficient ($\log D_{7.4}$), and Information for Each of the K15 Variants.

We began by investigating the effect of variable lipophilicity on the potency and toxicity of a previously identified antimicrobial peptoid, K15.²⁰ Synthesis of the variant species was performed on Rink Amide resin via peptoid submonomer methods²³ using bromoacetic acid, diisopropylcarbodiimide, and the appropriate amines. K15-13, K15-10, K15-8, K15-6, and K15-3 were synthesized using tridecylamine, decylamine, octylamine, hexylamine, and propylamine, respectively for the N-terminal submonomer (**Figure 3.3A**). K15-1, a single carbon tail variant was synthesized using traditional Fmoc solid-phase peptide methods²⁴ with Fmoc protected

sarcosine. All compounds were cleaved from the resin under acidic conditions, purified by RP-HPLC, and analyzed via mass spectrometry to confirm their respective structures (**Figures 3.4A-F**). Physicochemical properties of the K15 variants were computationally determined by ChemAxon's MarvinSketch Calculator Plugins (**Figure 3.3B**).²⁵ $\text{Log}D_{7.4}$, the diffusion coefficient at pH 7.4, was used as a descriptor of the variants lipophilicity (**Figure 3.3B**). The diffusion coefficient represents a molecule's preference for aqueous or lipophilic environments and provides predictive information about the bioavailability and partitioning of a potential drug molecule *in vivo*. These data correlate well with the percentage of less polar elution solvent (acetonitrile) during RP-HPLC purification, a second measure of hydrophobicity. Unsurprisingly, a linear correlation was observed between $\text{log}D_{7.4}$ and alkyl tail length of the variants (**Figure 3.5**).

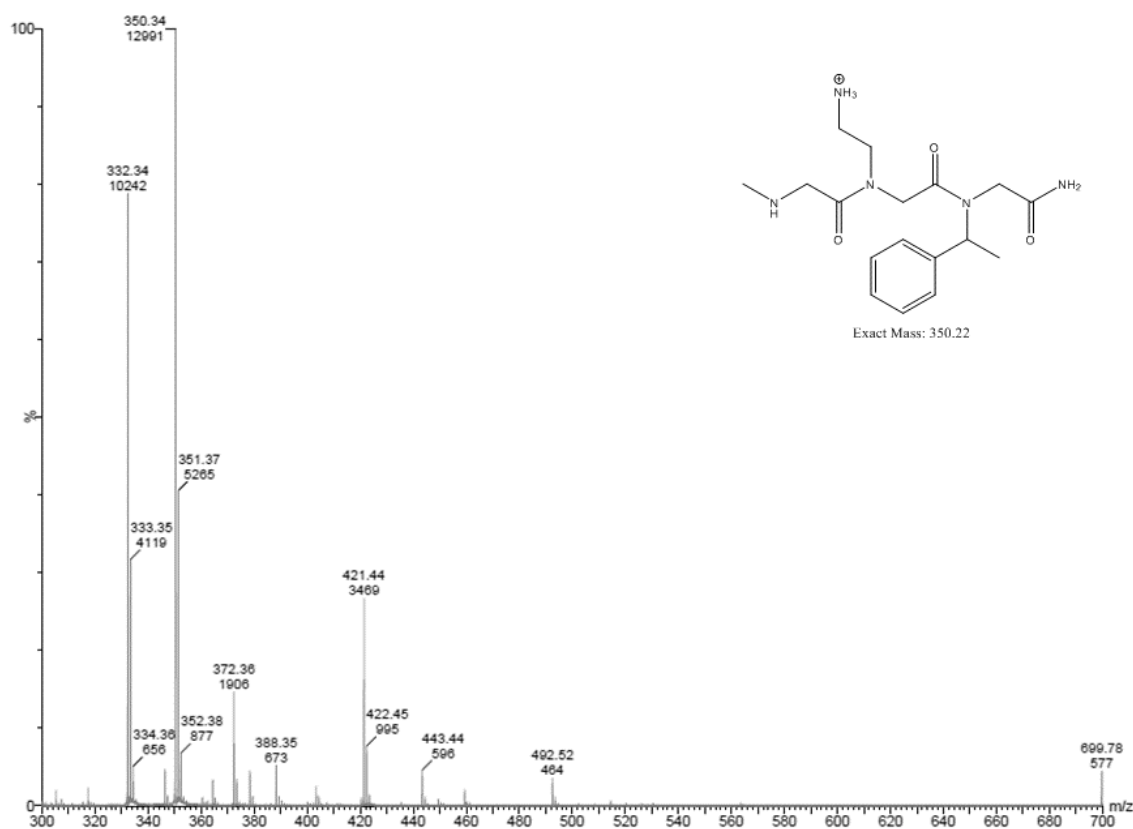


Figure 3.4A. Structure and Linear MS of K15-1.

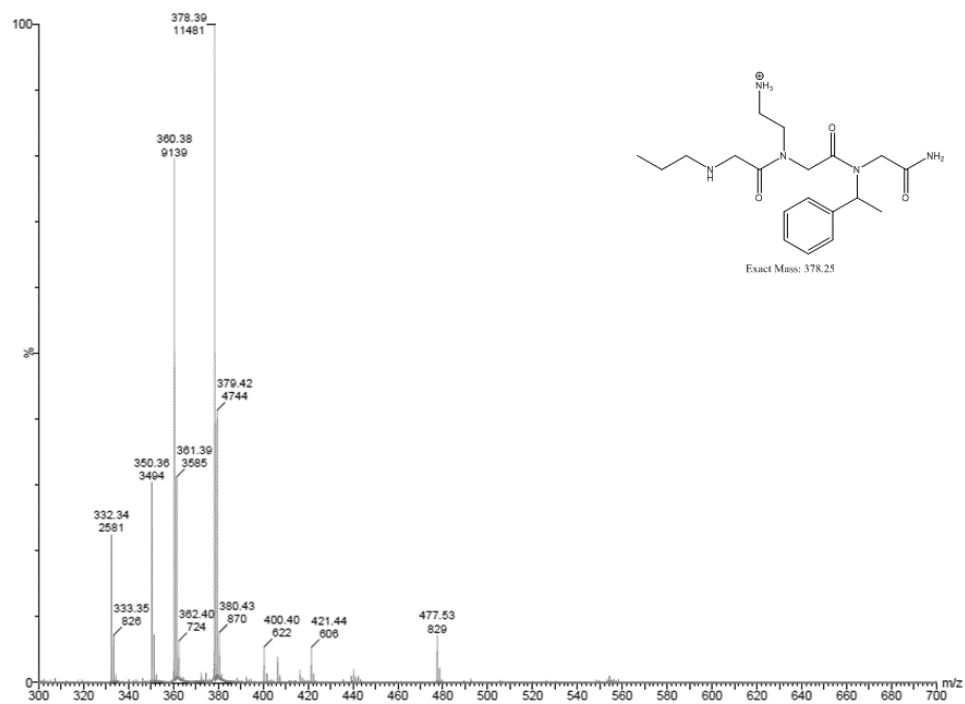


Figure 3.4B. Structure and Linear MS of K15-3.

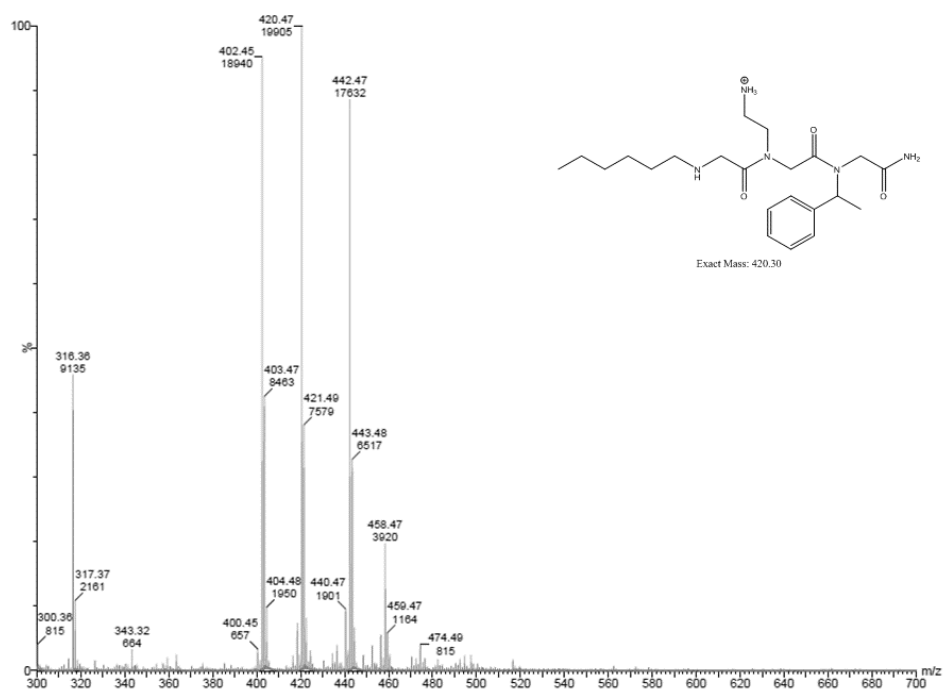


Figure 3.4C. Structure and Linear MS of K15-6.

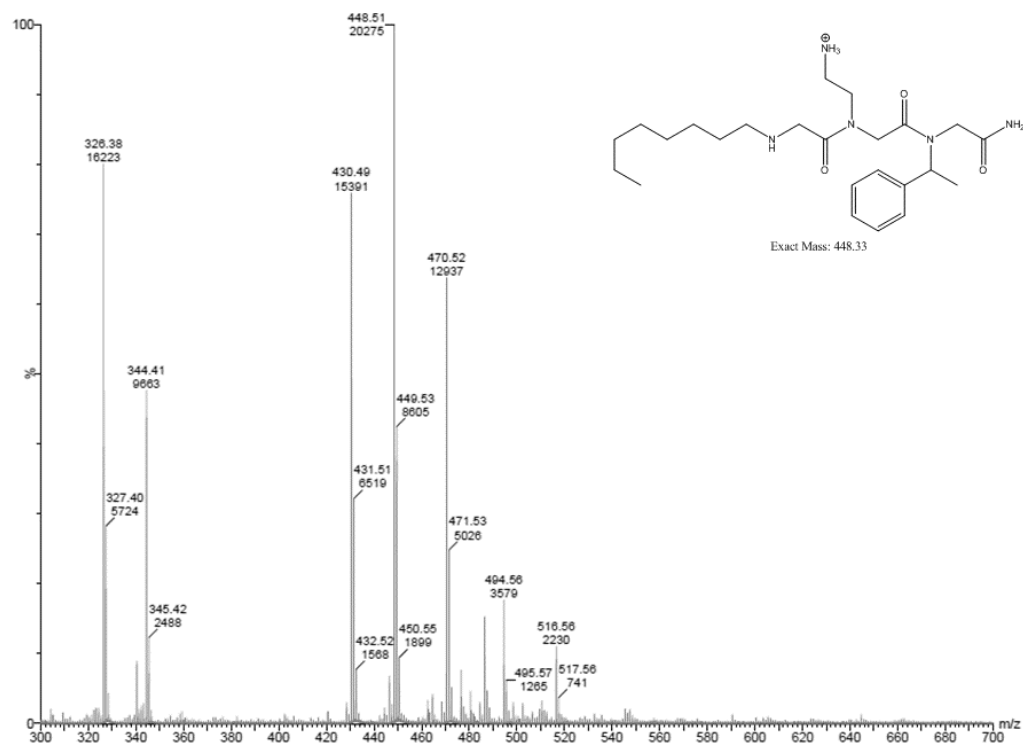


Figure 3.4D. Structure and Linear MS of K15-8.

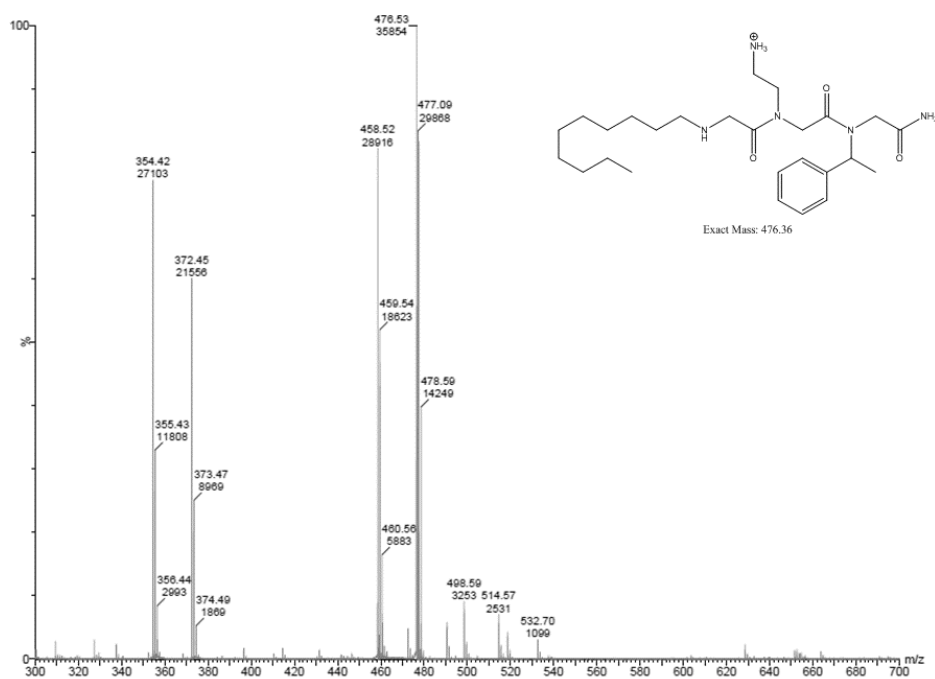


Figure 3.4E. Structure and Linear MS of K15-10.

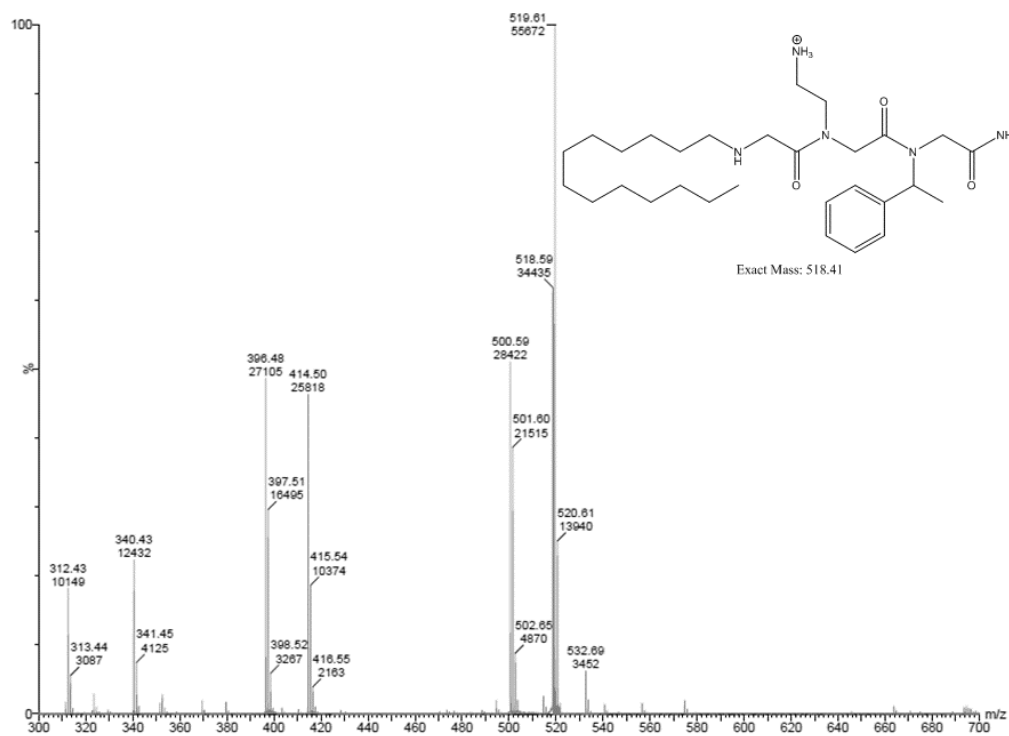


Figure 3.4F. Structure and Linear MS of K15-13.

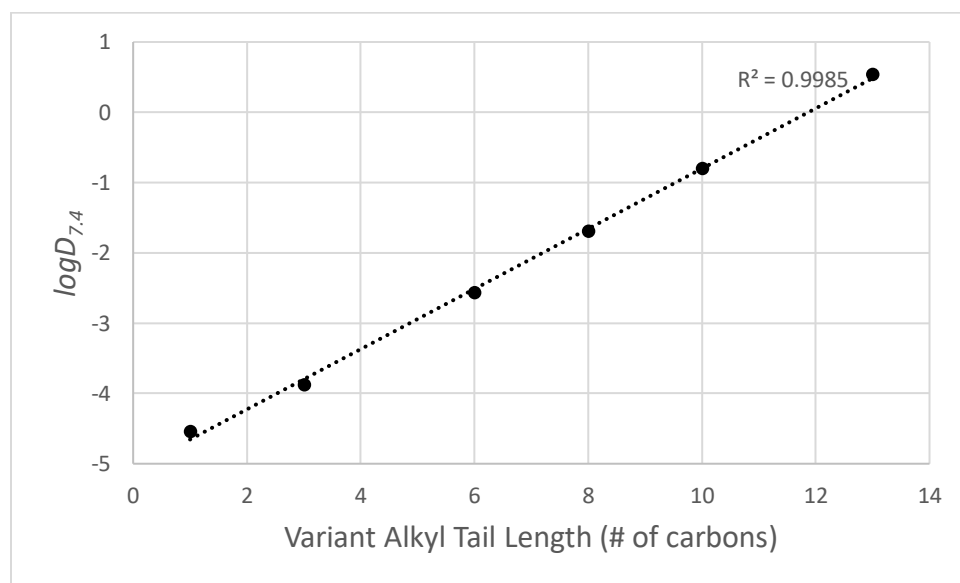


Figure 3.5. Correlation Between Variant Alkyl Tail Length and Calculated Diffusion Coefficient ($\log D_{7.4}$).

Antimicrobial potency of the variant compounds was determined by standard broth dilution against Gram-negative *A. baumannii* (ATCC 19606) and Gram-positive *E. faecalis* (ATCC 29212), microorganisms against which K15 had shown efficacy previously.²⁰ Significant reduction in bacterial growth of both pathogens was observed only by the two peptoids with the longest alkyl tails, K15-10 and K15-13 (**Table 1** and **Figure 3.6**). K15-13 exhibited minimum inhibitory concentrations (MICs) of 25 µg/mL and 6.3 µg/mL for *A. baumannii* and *E. faecalis*, respectively while K15-10 had MICs of 100 µg/mL and 50 µg/mL for *A. baumannii* and *E. faecalis*, respectively. K15 variants with alkyl tails shorter than 10 carbons did not exhibit any inhibition of bacterial growth even at the highest concentration tested, 800 µg/mL. The observation that Gram-positive bacteria were more susceptible to the antibacterial peptoids tested than Gram-negative bacteria is not surprising given that peptoids are hypothesized to exert antimicrobial activity through membrane targeting and disruption.²⁶ The membranes of Gram-positive bacterial are surrounded by a thick peptidoglycan multi-layer membrane, whereas Gram-negative microbes possess a lipid outer and inner membrane sandwiching a peptidoglycan membrane. The relative simplicity of Gram-positive membranes provides for greater permeation of small molecule drugs.²⁷

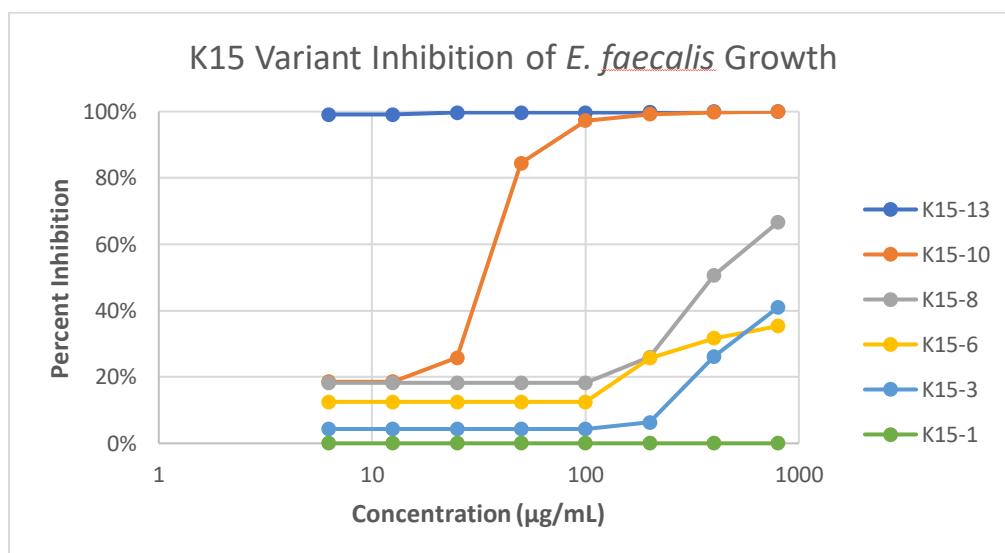
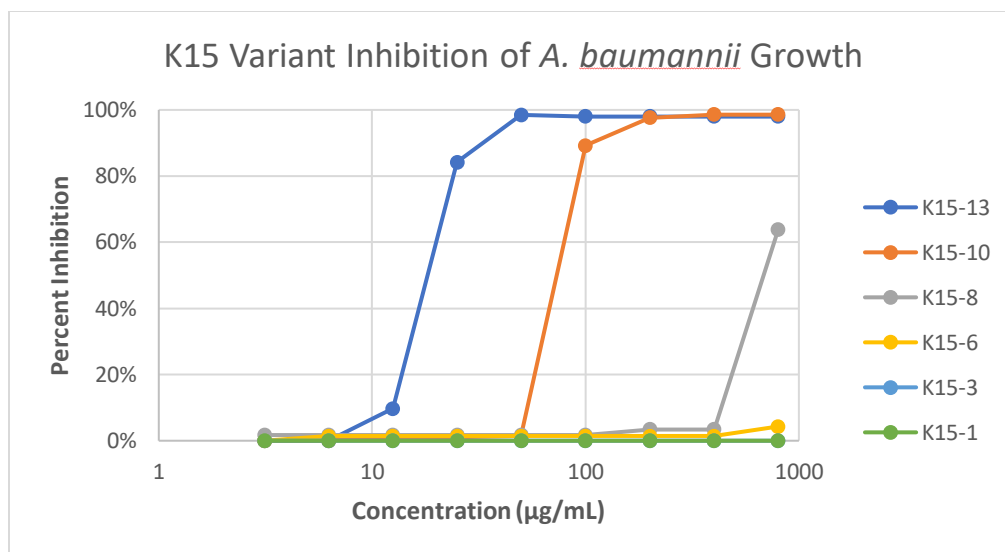


Figure 3.6. Growth Inhibition Profiles of the K15 Variants Against Gram-Negative *A. baumannii* and Gram-Positive *E. faecalis*.

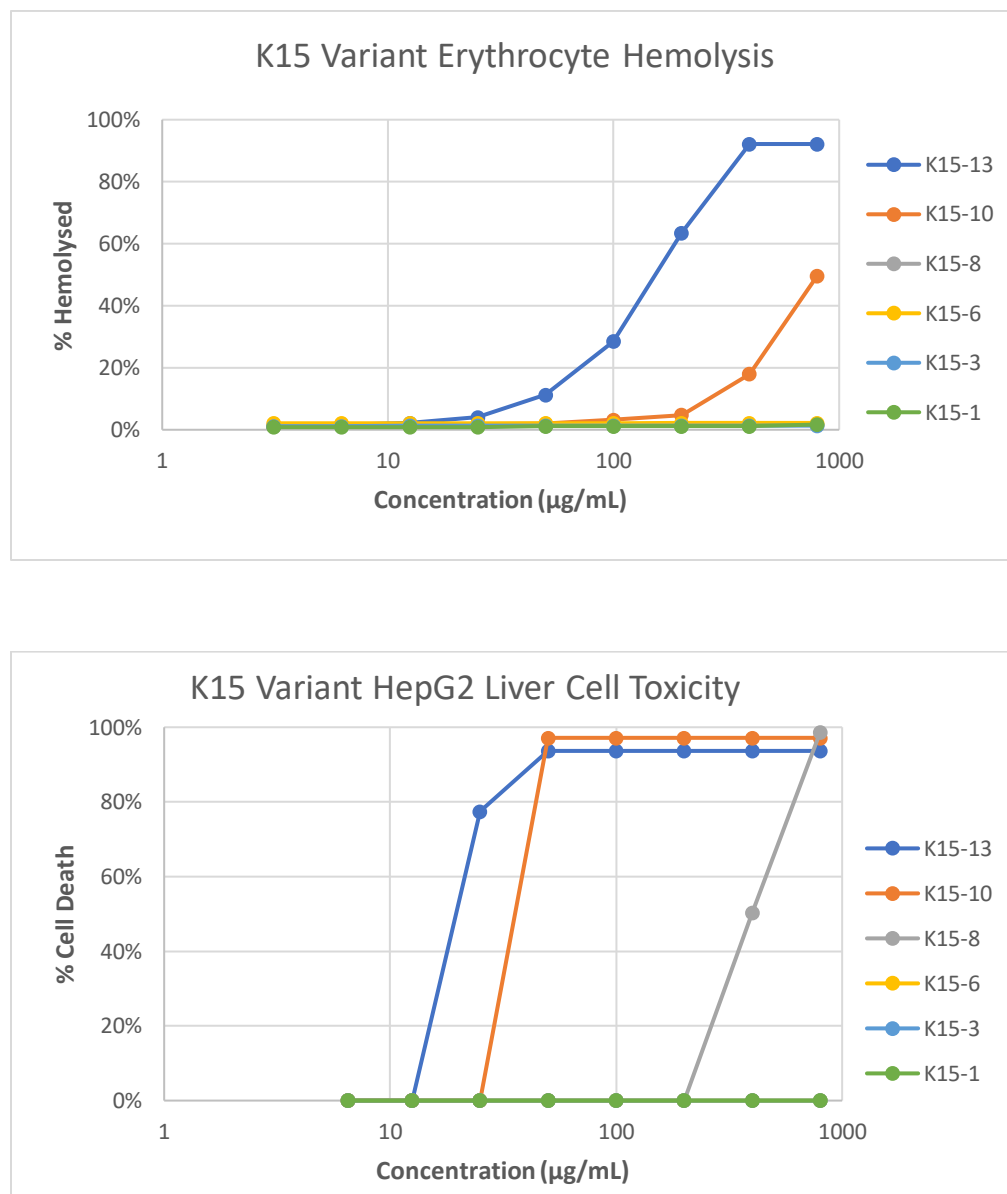


Figure 3.7. Toxicity Profiles of the K15 Variants Against Erythrocytes and HepG2 Hepatocellular Carcinoma Cells.

Cytotoxicity of the K15 variants was determined against HepG2 human hepatocellular carcinoma cells and human erythrocytes (**Table 1** and **Figure 3.7**). Concentrations ranging from

800-6.3 $\mu\text{g/mL}$ were assayed in 2-fold serial dilutions. As was observed for antimicrobial potency, alkyl tail length and lipophilicity correlated directly with toxicity. Decreased alkyl tail length resulted in decreased cytotoxicity as measured by the concentration at which 10% of the erythrocytes in the sample were lysed (HC_{10}) and concentration at which 50% of the HepG2 cells were nonviable (TD_{50}). It is important to note that a strong inverse relationship was observed between potency and toxicity. As alkyl tail length of the K15 variants increased, antimicrobial potency improved but toxicity became worse. Selectivity ratios (SR), a measurement of a compounds selectivity for pathogenic microbes over healthy cells, were calculated where possible (**Table 3.1**). The SRs calculated for K15-13 and K15-10 show narrow or no therapeutic window, seeming to effect bacteria and mammalian cells equally.

Table 3.1. Antibacterial Potency and Mammalian Cytotoxicity of K15 Variants

K15 Variant	MIC <i>A. baumannii</i> ($\mu\text{g/mL}$)	MIC <i>E. faecalis</i> ($\mu\text{g/mL}$)	HC_{10} ($\mu\text{g/mL}$)	Erythrocyte/ <i>A. baumannii</i> SR	Erythrocyte/ <i>E. faecalis</i> SR	HepG2 TD_{50} ($\mu\text{g/mL}$)	HepG2/ <i>A. baumannii</i> SR	HepG2/ <i>E. faecalis</i> SR
K15-13	25	6.3	14.80	0.59	2.3	20.33	0.81	3.2
K15-10	100	50	188.6	1.9	3.8	147.0	1.5	2.9
K15-8	>800	>800	>800	ND	ND	365.1	ND	ND
K15-6	>800	>800	>800	ND	ND	>800	ND	ND
K15-3	>800	>800	>800	ND	ND	>800	ND	ND
K15-1	>800	>800	>800	ND	ND	>800	ND	ND

MIC = minimum inhibitory concentration; HC_{10} = hemolysis concentration 10%; TD_{50} = toxic dose 50%; SR = selectivity ratio ($\text{TD}_{50}/\text{MIC}$); ND = not determined

Lipophilic Modification of JTL1

Having seen the impact of lipophilic modulation on both antimicrobial potency and cytotoxicity with a single peptoid compound, we next coupled alkyl tails of differing lengths (10 and 13) to JTL1, hypothesizing that increased library lipophilicity would increase hit rates. Recall that JTL1 was observed previously to be ineffective against bacteria in the PLAD assay. Synthesis was accomplished by coupling either tridecylamine or decylamine via submonomer methods⁷ to combinatorial peptoid libraries of identical length and submonomer composition to JTL1. This was done prior to deprotection of Boc groups from submonomer side-chain amino groups to assure lipidation of only the peptoid N-terminus. The PLAD assay was used to screen the functionalized libraries, termed JTL1₁₃ and JTL1₁₀ (**Figure 3.2**), along with the original JTL1 library against *S. aureus*, *E. faecalis*, and *A. baumannii* (**Figure 3.8**). The hit rate, defined as the number of beads exhibiting a measurable zone of inhibition out of the total number of beads screened, increased modestly for *S. aureus* from 0% for JTL1 to 3.3% for JTL1₁₀ and to 4.2% for JTL1₁₃ (**Figure 3.3C**). Although little difference in hit rate between the 10 carbon alkyl tail and 13 carbon alkyl tail was observed against *S. aureus*, this was not the case for these libraries against *E. faecalis* and *A. baumannii*. For *E. faecalis* the hit rate increased from 0% for JTL1 to 8.8% for JTL1₁₀ and to 16.7% for JTL1₁₃ while for *A. baumannii* the hit rate increased from 0% for JTL1 to 6.7% for JTL1₁₀ and to 16.6% for JTL1₁₃. For both of these microorganisms, the hit rate increased roughly two-fold when a 13 carbon alkyl tail was used instead of a 10 carbon alkyl tail, representing the significant increase in compound potency afforded by a relatively minimal lengthening of the lipophilic moiety. Note that while zones of complete clearance of bacterial growth were observed for *E. faecalis* and *A. baumannii*, only zones of reduced growth were ever observed for *S. aureus* (**Figure 3.8**), even with multiple PLAD screenings.

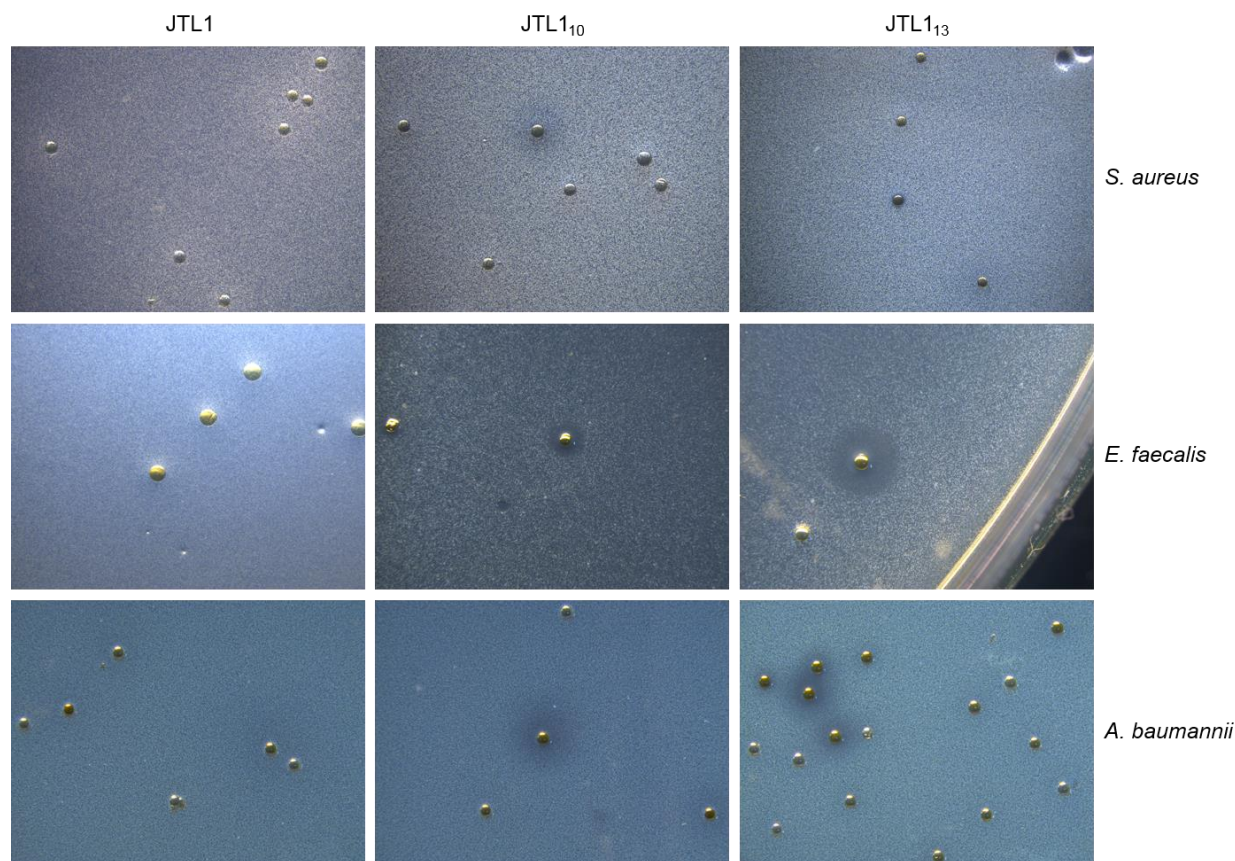


Figure 3.8. Representative Images of the PLAD Screenings of Libraries JTL1, JTL1₁₀, and JTL1₁₃ Against *S. aureus*, *E. faecalis*, and *A. baumannii*. Zones of Inhibition can be Observed Around Beads Displaying Antimicrobial Peptoids for Both JTL1₁₀ and JTL1₁₃ for All Three Pathogens Tested.

The observed link between alkyl tail length, increased antimicrobial potency, and concomitant increased unwanted cytotoxicity was disconcerting to our efforts to develop antimicrobial peptoids. However, a recently submitted study from our lab reports an antifungal compound, AEC5, which shares many chemical characteristics with K15-13, including a tridecyl tail, charged amino sidechain, and a bulky aromatic residue.²¹ AEC5 underwent the same cytotoxic assay cell panel, but showed considerably lower toxicity compared to K15-13 and K15-10, with HepG2 TD₅₀ and erythrocytes HC₁₀ values of 56.2 and 68.7 µg/mL, respectively. With an MIC

against *Cryptococcus neoformans* of 6.3 $\mu\text{g/mL}$, this gave AEC5 SR values of roughly 9 against HepG2 cells and 11 against erythrocytes, representing a significantly better therapeutic window than any of the K15 variants tested here. Interestingly, the $\log D_{7.4}$ for AEC5 was calculated to be -1.81, which is much closer to that of K15-8, -1.69, than the more structurally related K15-13, 0.54. This suggests that elevated $\log D_{7.4}$ correlates more accurately than longer alkyl tail length with a higher degree of mammalian cytotoxicity, and may therefore point to overall lipophilicity as being responsible for cytotoxicity of antimicrobial peptoids, not strictly alkyl tail length.

While the potency and toxicity of the studied antimicrobial peptoids show a limited therapeutic window, the effect of alkylating a combinatorial library to obtain higher hit rates has illuminated a potential direction for further investigation into rational library design of antimicrobial peptoids. The addition of a highly lipophilic moiety to a library of compounds can effectively activate those with latent antimicrobial potential. Toxicity, while seemingly tied to degree of alkylation in the present work, might be reduced by altering the randomized peptoid submonomers in a library to include more hydrophilic residues, rather than shortening the tail. This library design would maintain the long alkyl tail that this data suggests is important for antimicrobial activity, while reducing a peptoids overall $\log D_{7.4}$, which appears to be principally responsible for cytotoxicity.

Synthesis of JTL2

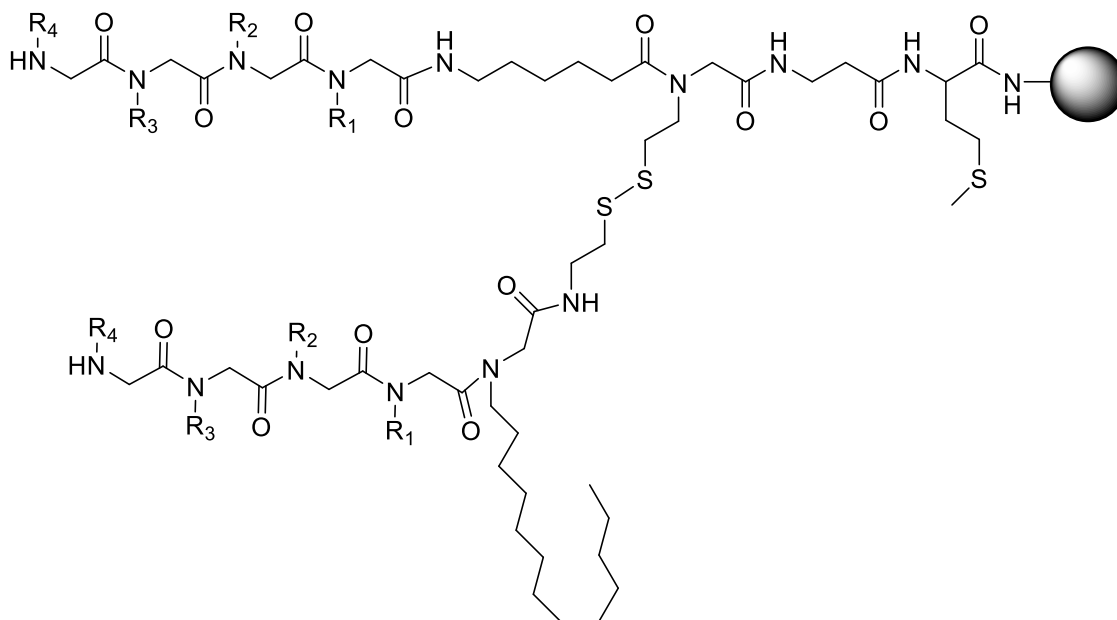


Figure 3.9. JTL2 Library Schematic, Showing Alkyl Tail Attached to *Beta*-strand Alone.

Many of the hits identified from JTL1₁₃ proved to be particularly difficult to sequence via ESI mass spectrometric analysis. It was hypothesized that the long carbon tail inhibited compound ionization and flight during mass spectrometric analysis. JTL2 (**Figure 3.9**) was designed with the intent of ameliorating the analytical obstacle presented by large lipophilic moieties. An aliquot of the TentaGel immobilized PLAD linker was treated with a TFA/TIS/water solution, removing the Boc protecting group from the *beta*-strand; while the Fmoc protecting group was left attached to the *alpha*-strand. The beads were then coupled to tridecylamine using peptoid submonomer methods.²³ The Fmoc group was removed by treatment with 20% piperidine in DMF (v/v). Next, the same combinatorial library composition as JTL1 was again used, resulting in a tetramer library of theoretical diversity 4096. In theory, by selectively deprotecting the linker molecule, the *beta*-strand would have the carbon tail which has been shown to be vital to the potency of peptoid antimicrobials, while the *alpha*-strand used in sequencing would be free of the moiety and

therefore be easier to analyze. However, after multiple PLAD screenings and the persistence of issues with MS analysis of the *alpha*-strand, it became apparent sequencing would be a significant challenge.

Synthesis of JTL3

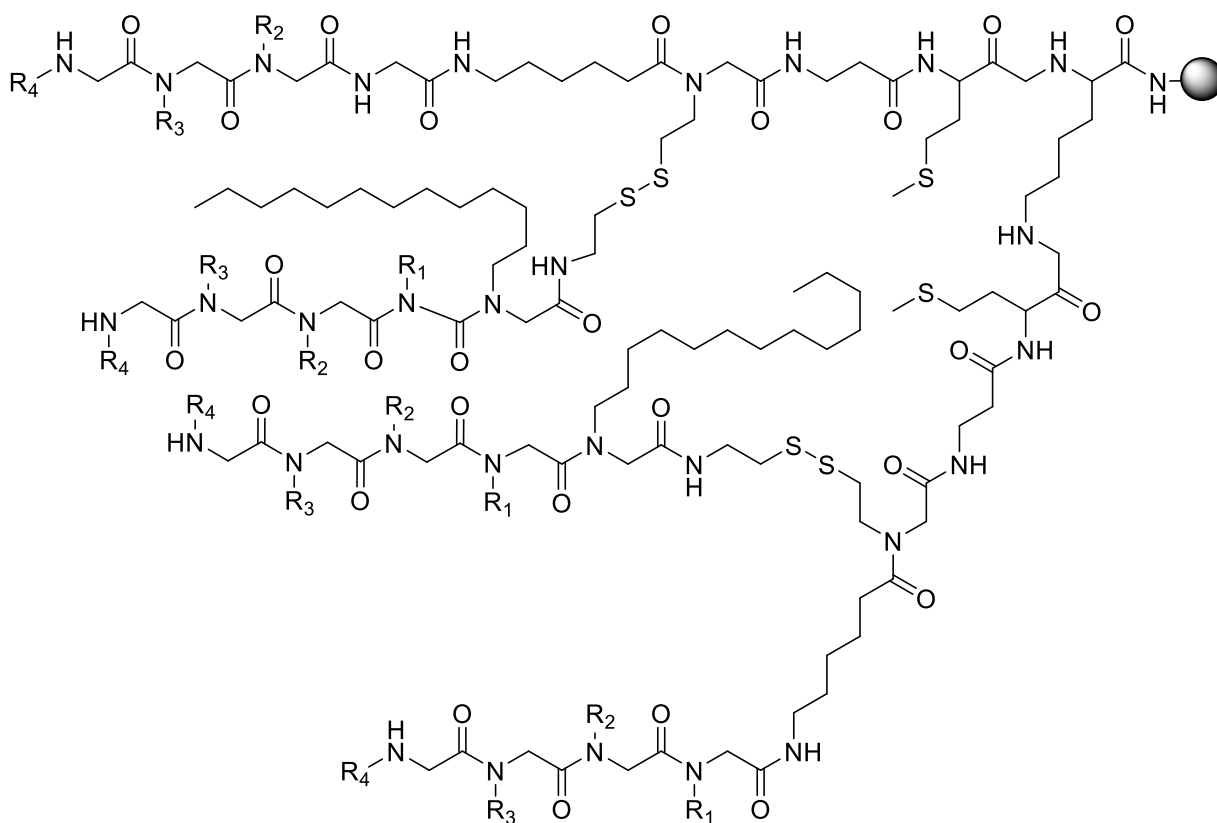


Figure 3.10. JTL3 Library Schematic, Showing Two Disulfide Linker Molecules Anchored to the Bead by a Lysine Residue.

JTL3 built upon the “tail first” approach of JTL2 with the additional modification of doubling the number of *alpha*- and *beta*-strands (**Figure 3.10**). This was accomplished by coupling an aliquot of TentaGel macrobeads to a COMU activated lysine(MTT) residue. The lysine was

deprotected of MTT by a 1% TFA in DMF (v/v) solution and Fmoc by 20% piperidine in DMF (v/v), allowing synthesis to take place on both amines. Synthesis of the disulfide linker was performed as recorded. The *beta*-strand was deprotected by treatment with a TFA/TIS/water solution, resulting in the removal of the Boc protecting group. Tridecylamine was coupled via peptoid submonomer methods²³ to the deprotected *beta*-strand, followed by the deprotection of the *alpha*-strand by 20% piperidine in DMF (v/v). The same combinatorial library composition as JTL1 was used for a tetramer library of theoretical diversity 4096. The resultant library would effectively have double the concentration of JTL1 and JTL2 by the nature of the di-amine of anchored lysine. The effect of this added concentration was noted in an increased visibility of zones of inhibition in PLAD assay screening, yet successful sequencing was not achieved.

Synthesis of Arginine Mimic

Diversity of amine side-chains incorporated into antimicrobial peptoids has been hitherto limited. We sought to include a novel amine in our libraries. An arginine mimic was of particular interest as charged residues in peptoids were limited to di-amines. We first sought to functionalize 1,3-diaminopropane with *N,N'*-bis(tert-butoxycarbonyl)-1H-pyrazole-1-carboxamide by slow addition with diisopropylethylamine in THF. The product yielded an unexpected MS showing a peak at 200.25 and 100.25 (corresponding to the loss of a Boc protecting group) rather than the expected 317.40, 217.40, and 117.40 m/z. NMR confirmed cyclization of the desired product (**Figure 3.11**). A similar phenomenon had been observed by Castagnolo *et al.* in attempts to synthesize the propyl product.

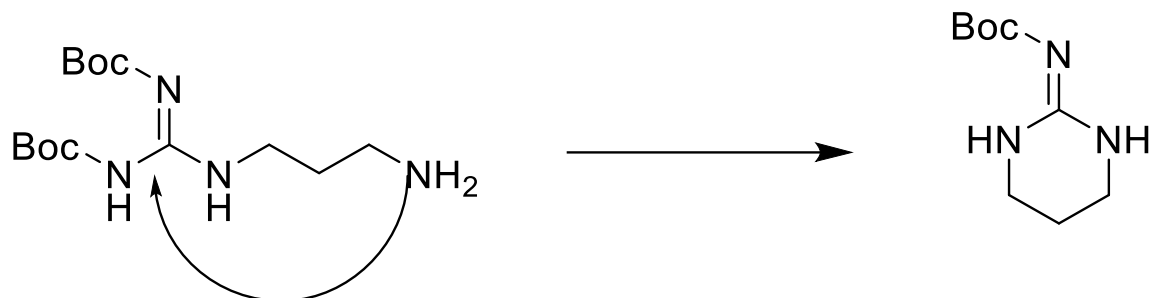


Figure 3.11. Cyclization of Propyl Di-Amine Arginine Mimic.

We then decided to shorten the di-amine chain to 1,2-diaminoethane, reasoning that cyclization would be hindered as a preferred six-membered ring could not result. Reaction conditions were kept constant, and the resulting product analyzed via MS. Peaks at 303.38, 203.38, and 103.38 *m/z* confirmed the desired product (**Figure 3.12**). The amine will feature in a structure activity relationship study with a focus on novel amine side-chains.

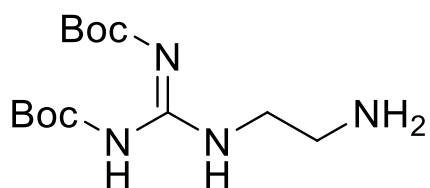


Figure 3.12. N-(aminoethyl)-N'-N''-bis-(*tert*-butoxycarbonyl)guanidine)

CHAPTER FOUR: CONCLUSION

The thesis presented sought to probe the importance of lipophilicity and alkylation of our libraries in screening for antimicrobial activity. Determination of K15 variant antimicrobial potency and cytotoxicity, taken with the characterization of AEC5, has illuminated a $\log D_{7.4}$ range in which specificity is theorized to favor bacterial membrane interaction. It is also of import to note the alkyl tail is tied to efficacy. With this knowledge, we are better able to design potent compound libraries with specificity for bacterial membrane interactions. The study which was herein described led to a change in library design, briefly the alkylation of the library, which has observably improved hit rate. Within this work, the PLAD assay was optimized for use against each of the ESKAPE pathogens. Given the ease with which the assay was adapted to the varied microbes, expansion to other bacteria seems to be limited only by the ability for the organism to yield a uniform lawn. Future work will include a detailed structure activity relationship of novel amine side-chains. The PLAD assay has been shown capable of screening large diversity libraries against an array of pathogens. Sequencing remains an obstacle, however techniques such as DNA encoded libraries have been suggested as potential solutions. The next direction for PLAD assay development is application to mammalian cell lawns, in effect allowing for rapid screening of library toxicity. This would provide another metric by which studies of library physicochemical properties may be measured.

REFERENCES

- (1) Fisher, K. J.; Turkett, J. A.; Corson, A. E.; Bicker, K. L. Peptoid Library Agar Diffusion (PLAD) Assay for the High-Throughput Identification of Antimicrobial Peptoids. *ACS Comb. Sci.* **2016**, *18* (6), 287–291.
- (2) Turkett, J. A.; Bicker, K. L. Evaluating the Effect of Peptoid Lipophilicity on Antimicrobial Potency, Cytotoxicity, and Combinatorial Library Design. *ACS Comb. Sci.* **2017**, *19* (4), 229–233.
- (3) Demain, A.; Sanchez, S. Microbial Drug Discovery: 80 Years of Progress. *J. Antibiot. (Tokyo)* **2009**, *62*, 5–16.
- (4) Bush, K. Antimicrobial Agents Targeting Bacterial Cell Walls and Cell Membranes. *Rev. Sci. Tech.* **2012**, *31* (1), 43–56.
- (5) Brogden, K. Antimicrobial Peptides: Pore Formers or Metabolic Inhibitors in Bacteria? *Nature* **2005**, *3*, 238–250.
- (6) *Antimicrobial Resistance: Report on Global Surveillance*; World Health Organization: France, 2014.
- (7) Neu, H. The Crisis in Antibiotic Resistance. *Science* **1992**, *257*, 1064–1073.
- (8) Andreu, D.; Rivas, L. Animal Antimicrobial Peptides: An Overview. *Biopolymers* **1998**, *47* (6), 415–433.
- (9) Hancock, R.; Sahl, H. Antimicrobial and Host-Defense Peptides as New Anti-Infective Therapeutic Strategies. *Natl. Biotechnol.* **2006**, *24* (12), 1551–1557.
- (10) Zasloff, M. Antimicrobial Peptides of Multicellular Organisms. *Nature* **2002**, *415*, 389–395.

- (11) Giuliani, A.; Rinaldi, A. Beyond Natural Antimicrobial Peptides: Multimeric Peptides and Other Peptidomimetic Approaches. *Cell Mol Life Sci* **2011**, *68* (13), 2255–2266.
- (12) Miller, S.; Simon, R.; Simon, N.; Zuckermann, R.; Kerr, J.; Moos, W. Proteolytic Studies of Homologous Peptide and N-Substituted Glycine Peptoid Oligomers. *Bioorg. Med. Chem. Lett.* **1994**, *22*, 2657–2662.
- (13) Kapoor, R.; Eimerman, P.; Hardy, J.; Barron, A. Efficacy of Antimicrobial Peptoids against Mycobacterium Tuberculosis. *Antimicrob. Agents Chemother.* **2011**, *55* (6), 3058–3062.
- (14) Kapoor, R.; Wadman, M.; Dohm, M.; Barron, A. Antimicrobial Peptoids Are Effective against Pseudomonas Aeruginosa Biofilm. *Antimicrob. Agents Chemother.* **2011**, *55* (6), 3054–3057.
- (15) Areum Shin; Young-Guen Park; Jeong Kyu Bang; Dasom Jeon; Eunjung Lee; Yong-Sun Park; Song Yub Shin; Yangmee Kim. Peptoid-Substituted Hybrid Antimicrobial Peptide Derived from Papiliocin and Magainin 2 with Enhanced Bacterial Selectivity and Anti-Inflammatory Activity. *Biochemistry (Mosc.)* **2015**, No. 25, 3921.
- (16) Chongsiriwatana, N.; Patch, J.; Czyzewski, A.; Dohm, M.; Ivankin, A.; Gidalevitz, D.; Zuckermann, R.; Barron, A. Peptoids That Mimic the Structure, Function, and Mechanism of Helical Antimicrobial Peptides. *Proc Natl Acad Sci USA* **2008**, No. (8); 02, 2008.
- (17) Zuckermann, R.; Kerr, J.; Kent, S.; Moos, W. Efficient Method for the Preparation of Peptoids [oligo(N-Substituted Glycines)] by Submonomer Solid-Phase Synthesis. *J. Am. Chem. Soc.* **1992**, *114* (26), 10646–10647.
- (18) Fenniri, H. *Combinatorial Chemistry: A Practical Approach*; The Practical Approach Series; Oxford University Press: Oxford, 2000.

- (19) Kennedy, J.; Williams, L.; Bridges, T.; Daniels, R.; Weaver, D.; Lindsley, C. Application of Combinatorial Chemistry Science on Modern Drug Discovery. *J. Comb. Chem.* **2008**, *10* (3), 345–354.
- (21) Corson, A. E.; Armstrong, S. A.; Wright, M. E.; McClelland, E. E.; Bicker, K. L. Discovery and Characterization of a Peptoid with Antifungal Activity against *Cryptococcus Neoformans*. *ACS Med. Chem. Lett.* **2016**, *7* (12), 1139–1144.
- (22) Chongsiriwatana, N.; Miller, T.; Wetzler, M.; Vakulenko, S.; Karlsson, A.; Palecek, S.; Mobashery, S.; Barron, A. Short Alkylated Peptoid Mimics of Antimicrobial Lipopeptides. *Antimicrob. Agents Chemother.* **2011**, *55* (1), 417–420.
- (23) Zuckermann, R.; Kerr, J.; Kent, S.; Moos, W. Efficient Method for the Preparation of Peptoids [oligo(N-Substituted Glycines)] by Submonomer Solid-Phase Synthesis. *J. Am. Chem. Soc.* **1992**, *114* (26), 10646–10647.
- (24) Amblard, M.; Fehrentz, J.-A.; Martinez, J.; Subra, G. Methods and Protocols of Modern Solid Phase Peptide Synthesis. *Mol. Biotechnol.* **2006**, No. 3, 239.
- (25) *MarvinSketch*.
- (26) Brogden, K. Antimicrobial Peptides: Pore Formers or Metabolic Inhibitors in Bacteria? *Nature* **2005**, *3*, 238–250.
- (27) Brown, L.; Wolf, J. M.; Prados-Rosales, R.; Casadevall, A. Through the Wall: Extracellular Vesicles in Gram-Positive Bacteria, Mycobacteria and Fungi. *Nat. Rev. Microbiol.* **2015**, *13* (10), 620–630.